FINAL REPORT

TEN MICRON WIDEBAND DETECTOR

CONTRACT No. N00014-70-C-022

30 SEPTEMBER 197

J. Fa
J.M. Yarboroug

Prepared f

THE OFFICE OF NAVAL RESEARCH WASHINGTON, D.

RECONNAISSANCE ■ ELECTRONIC WARFARE ■
SECURITY/SURVEILLANCE ■ SOCIOSYSTEMS
ELECTRO-OPTICS

GTE SYLVANIA
INCORPORATE
ELECTRONIC SYSTEMS GROUP/WESTERN DIVISIO

TEN MICRON WIDEBAND DETECTOR

FINAL REPORT

CONTRACT N00014-70-C-0224

30 September 1971

J. Falk

J. M. Yarborough

Prepared for
The Office of Naval Research
Washington, D.C.

FINAL REPORT

ARPA ORDER NUMBER:	306
PROGRAM CODE NUMBER:	0014
CONTRACTOR:	SES-WD
EFFECTIVE DATE:	1 April 1970
CONTRACT AMOUNT:	$99,807
CONTRACT:	N00014-70-C-0224
PROJECT SCIENTIST:	J. M. Yarborough
TELEPHONE:	(415) 966-3710
TITLE:	10 MICRON WIDEBAND DETECTOR

This research was supported by the Advanced Research Projects Agency of Department of Defense and was monitored by the Office of Naval Research under Contract No. N00014-70-C-0224.

ABSTRACT

This report summarizes the results obtained during a sixteen month parametric upconversion program. The goal of the program was the visualization of a thermal image via parametric upconversion. Toward that end a theoretical and experimental effort was undertaken. The theory of parametric upconversion was extended to describe the detection of a thermal image by frequency conversion. The theory developed describes the power output, resolution, contrast and spectral bandwidth to be expected from a thermal upconverter.

Experimentally, the first detection via parametric upconversion of thermal radiation from a room temperature blackbody source was achieved, providing confirmation of the theory developed. Efforts at viewing an upconverted thermal scene were not successful due to the limited damage resistance of the nonlinear material, proustite, and the poor performance of the InAsP image tube that was used to view the upconverter output.

FOREWORD

This report summarizes the work performed on ONR Contract N00014-70-C-0224 entitled "Ten Micron Wideband Detector". The goal of this program was to investigate 8 to 13 micron blackbody image upconversion. The work detailed in this report covers the period April 1, 1970 to July 30, 1971. This report was prepared by the Electro-Optics Organization of GTE Sylvania, Inc., Electronic Systems Group, Mountain View, California, and describes work performed in the Research and Development Department headed by Dr. L. M. Osterink. The major technical contributors to this program were Drs. Joel Falk, and J. Michael Yarborough. Drs. Eugene O. Ammann, Joseph D. Taynai and William B. Tiffany were also contributors.

The research performed on this program was supported by the Advanced Research Projects Agency of the Department of Defense and was monitored by the Office of Naval Research. Dr. Fred Quelle is the contract monitor for this program.

TABLE OF CONTENTS

LIST OF FIGURES

LIST OF FIGURES

Section 1

INTRODUCTION

The potential advantages of infrared viewing have long been appreciated. Although much effort has been directed toward development of direct IR image detection scanning devices, very little work has been done on real-time systems. Scanning imaging systems currently employed require cryogenic cooling, are unable to store images and require awkward image scanning mechanisms. The disadvantages of these systems can be overcome by real-time conversion of infrared images to the visible or near-IR where high resolution, high gain image intensifiers exist. Optical parametric upconversion offers a method for performing this transformation. This process, the nonlinear coupling of an infrared signal of frequency ω_i with a strong laser beam of frequency ω_p, gives rise to an upconverted signal at the sum frequency $\omega_i + \omega_p = \omega_s$. It has been noted by many authors[1-9] that optical parametric upconversion is potentially capable of high-resolution, sensitive infrared image detection without the need for extreme cooling. An input signal for such image upconversion can be accomplished by illuminating a target with an infrared source or by collecting the black body radiation emitted by the target. For all but very high power illumination, collection of blackbody radiation should provide higher upconverted image intensities.

This report details efforts directed toward viewing a thermal scene by means of parametric upconversion. A three part experimental program was undertaken, starting with the mixing of 10.6 micron CO_2 with 1.06 micron Nd:YAG, proceeding to detection, via parametric frequency conversion of a hot blackbody source, and culminating with attempts to observe an upconverted thermal image.

This report reviews the theory of upconversion of a coherent source and describes upconversion of CO_2 laser radiation. The existing upconverter theory is extended to describe blackbody-image upconversion. The theory developed includes a description of the expected power output from such an upconverter, its potential resolution, contrast, and spectral bandwidth. The first detection via parametric upconversion of thermal radiation emitted from a room temperature blackbody source is described, providing partial confirmation of the theory.[10] Although thermal upconversion attempts were successful, efforts at viewing an upconverted image were not. Image upconversion was prevented by poor image tube performance as well as the lack of laser damage resistance of the upconverter nonlinear material, proustite. Attempts at upconversion are described in detail. Suggestions for further image upconversion studies are presented. It is shown that with expected development of existing nonlinear materials[11] and image detectors[12] high resolution thermal image conversion may soon be possible.

Section 2

THEORY OF PARAMETRIC UPCONVERSION

Parametric upconversion is the mixing of radiation at radian frequencies ω_{idler} and ω_{pump} to produce energy at the sum or signal frequency $\omega_s = \omega_i + \omega_p$. This mixing, accomplished internal to a crystal having appreciable nonlinear properties, may be used as a mechanism for transferring radiation from the 10-micron region of the spectrum where poor detectors exist to the visible or near visible where better detectors are available. We will consider theoretically the interaction of three electromagnetic waves, called the signal, idler and pump, coupled together in a nonlinear medium by a nonlinear polarization (Figure 2-1). The pump for a parametric upconverter is in general a strong laser field. The idler wavelength is the upconverter input and the signal is the output of the upconverter. The starting point for our analysis will be the one dimensional Maxwellian wave equation driven by a polarization quadratic in electric field.[13] We consider the case where the nonlinear crystal is transparent at all relevant wavelengths, i.e., we examine the interaction of signal, idler and pump fields which obey the equation:

$$\frac{\partial^2 E}{\partial z^2} - \mu_o \varepsilon \frac{\partial^2 E}{\partial t^2} = \mu_o \frac{\partial^2 P}{\partial t^2} \qquad (2\text{-}1)$$

where μ_o and ε are the permeability and permitivity of the nonlinear medium.

A good understanding of the interaction involved may be gained by consideration of the case where all electromagnetic radiation present within

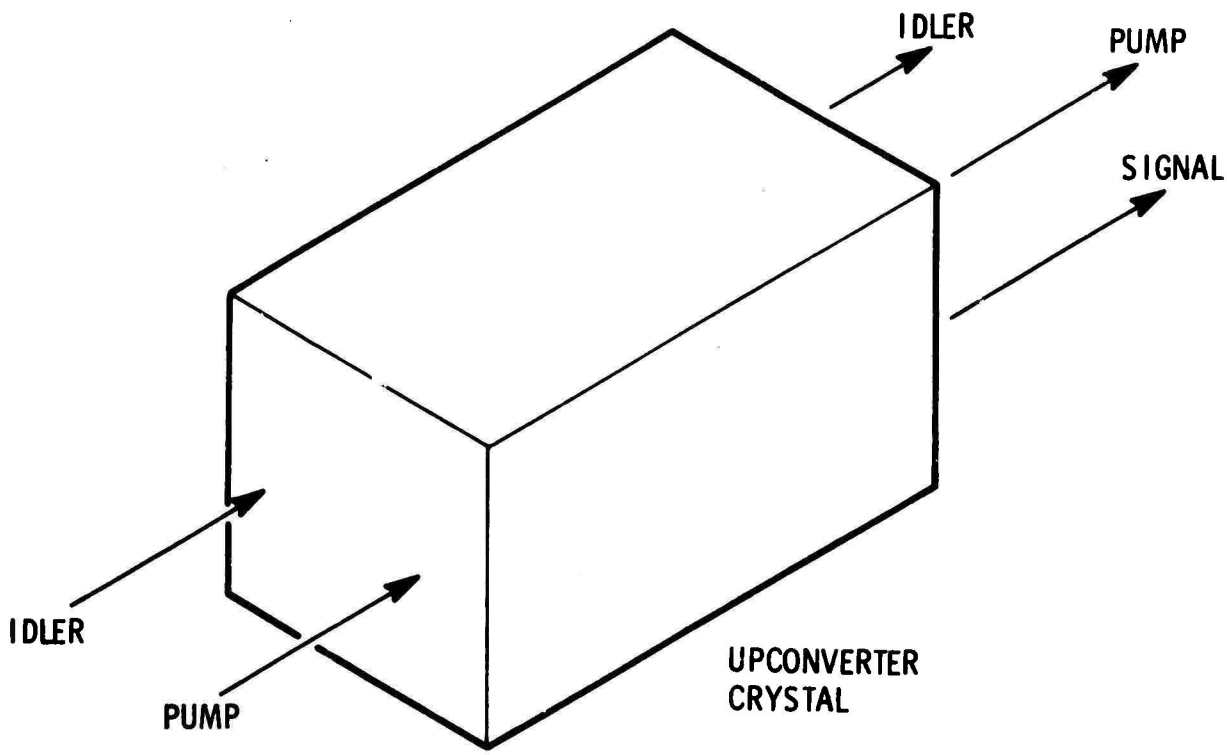

Figure 2-1 The parametric upconverter. Inputs are idler and pump fields. Outputs are signal, idler and pump fields.

the nonlinear medium exists as plane waves. While this is clearly not a precise physical possibility due to the infinite energy and lack of diffraction of a plane wave, a mathematical development based on plane wave theory will point out many of the significant attributes of the parametric upconverter. Further, although a plane wave situation is not precisely experimentally achievable, it is well approximated by loosely focused idler and pump beams.

Plane wave signal, idler and pump polarizations within nonlinear medium may be described by

$$P_n = \mathrm{Re}[P_n \exp (\omega_n t - k_n z)] \quad \text{where} \quad n = i, s, p . \tag{2-2a}$$

Similarly electric fields are described by

$$E_n(z,t) = \mathrm{Re}\,[E_n \exp j(w_n t - k_n t)] \quad n = i,s,p . \tag{2.2b}$$

We will consider these waves to be coupled together by nonlinear polarizations described phenomenologically by

$$P_s = dE_p E_i$$

$$P_i = dE_s E_p^*$$

$$P_p = dE_s E_i^*$$

where * denotes complex conjugate and where d is a nonlinear coefficient whose physical basis is discussed in detail in the literature.[14,15]

The Maxwell wave equation will be solved subject to the following conditions,

(1) Undepleted pump; $|E_p|$ = constant.

It is assumed that the pump field amplitude does not decay with distance propagated in the crystal. This implies that the parametric process removes an insignificant amount of energy from the pump.

(2) Idler and signal amplitudes vary slowly in space. It is a convenient mathematical, and physically sensible, assumption to consider spatial variations of the idler and signal that are much less than their respective wavevectors. Mathematically this implies

$$\left|\frac{\partial E_i}{\partial z}\right| \ll |k_i E_i| \tag{2-3}$$

$$\left|\frac{\partial E_s}{\partial z}\right| \ll |k_s E_s| \quad . \tag{2-4}$$

(3) Steady state. It is assumed that the electric field amplitudes do not vary in time, i.e. $\frac{\partial E_s}{\partial t} = \frac{\partial E_i}{\partial t} = \frac{\partial E_p}{\partial t} = 0.$

All changes in field amplitudes are assumed to be due to spatial variations. Substituting equations (2-2) into (2-1), subject to conditions (2-3) and (2-4), it is found that the Maxwell wave equation reduces to two simple equations describing the spatial variation of the signal and idler field amplitudes. These equations, known as the coupled mode equations, are:

$$\frac{\partial E_s}{\partial z} = - j\kappa_s E_i \exp j\Delta kz \tag{2-5}$$

$$\frac{\partial E_i}{\partial z} = - j\kappa_i^* E_s \exp - j\Delta kz \tag{2-6}$$

where $\kappa_s = \mu c_s \frac{\omega_s}{2} dE_p$, $\kappa_i = \mu c_i \frac{\omega_i}{2} dE_p$

$\Delta k = k_s - k_p - k_i$ and c_s and c_i

are the phase velocities at the signal and idler wavelengths, respectively. Equations (2-5) and (2-6) are sufficient to provide an implicit description of the operation of a parametric upconverter.

The usual upconverter (Fig. 2-1) has a weak idler input due to black body radiation or illumination in the ten micron spectral region and no input at the signal wavelength. Denoting the idler input by E_{10} and assuming zero signal input, we find that output signal power density may be determined from

$$E_s E_s^* = |\kappa_s \ell|^2 \, |E_{10}|^2 \left[\frac{\sin \sqrt{\kappa_i^* \kappa_s + (\frac{\Delta k}{2})^2} \; \ell}{\sqrt{\kappa_i^* \kappa_s + (\frac{\Delta k}{2})^2} \; \ell} \right]^2 . \qquad (2\text{-}7)$$

We note that the maximum output from the upconverter occurs with

$$\ell = \frac{\pi}{2\sqrt{\kappa_s \kappa_i^* + (\frac{\Delta k}{2})^2}}$$

and is given by

$$E_s E_s^* = \frac{\kappa_s^2}{\kappa_s \kappa_i^* + (\frac{\Delta k}{2})^2} \, |E_{10}|^2 \qquad (2\text{-}8)$$

If the upconversion of a coherent source, in a phasematchable material, is considered $\Delta\kappa$ can be adjusted to equal zero and (2-8) becomes a restatement of the well-known Manley-Rowe relationship.

It is easily shown from equation (2-7) that the power output from a phasematched "coherent" upconverter is given by

$$\frac{dP_s}{dA} = \frac{\kappa_s}{\kappa_i} \frac{\eta_i}{\eta_s} \frac{dP_i}{dA} \sin^2 \sqrt{\kappa_i \kappa_s} \; \ell \qquad (2\text{-}9)$$

where η_i and η_s are the crystalline electromagnetic impedances evaluated at the idler and signal frequencies respectively, P_i is the idler input power and A is the cross sectional area of the signal beam. In writing eq. (2-9) we have implicitly assumed that $\frac{dP_i}{dA}$ is independent of ℓ. This will be true for all situations considered in this report. If $\frac{dP_i}{dA}$ is a function of ℓ then the right hand side of equation (2-9) must be replaced by an integration over ℓ. For small parametric gains $\sqrt{\kappa_i \kappa_s}\ \ell \ll 1$ and (2-9) becomes,

$$P_s = \int (\kappa_s \ell)^2 \frac{\eta_i}{\eta_s} \frac{dP_i}{dA} dA \qquad (2\text{-}10)$$

where the integral is evaluated over the crystal cross sectional area.

Experimental verification of equation (2-10) is given in section 4 of this report. Here it suffices to note that equation (2-10) gives an estimation of the output of a coherent upconverter when diffraction and double refraction are negligible. More precise analyses are available for some upconverter configurations if diffraction or double refraction is important. Some further details of these analyses are given in section 4 of this report as well as in reference 15.

If the idler input is not coherent, i.e., if it is due to blackbody radiation or other radiation of wide spectral content, phase matching will not be possible over a large bandwidth, and in general $\left| \frac{\Delta k}{2} \right|^2 \gg \kappa_i^* \kappa_s$. Subject to this approximation the signal power output intensity from a blackbody, or "incoherent" upconverter is given by

$$I_s = \frac{\eta_i}{\eta_s} \left| \kappa_s \ell \right|^2 I_i \operatorname{sinc}^2 \frac{\Delta k \ell}{2} \qquad (2\text{-}11)$$

where we have written

$$I_s = \frac{dP_s}{dA} = \frac{E_s E_s^*}{\eta_s} \quad , \quad I_i = \frac{dP_i}{dA} = \frac{E_{10} E_{10}^*}{\eta_i}$$

and where

$$\text{sinc}^2 \frac{\Delta k \ell}{2} = \frac{\sin^2 \frac{\Delta k \ell}{2}}{(\frac{\Delta k \ell}{2})^2}$$

is the asynchronism or gain-line function commonly associated with low gain parametric interactions. [16]

Section 3

BLACKBODY UPCONVERSION

3.1 THEORETICAL CONSIDERATIONS

In this section we will consider the theoretical requirements for viewing thermal images in the 10 micron region via parametric upconversion. Expressions will be derived for the power and resolution to be expected from a parametric blackbody image upconverter constructed using a Nd:YAG laser and a proustite nonlinear crystal. It will be shown that resolution of a thermal image upconverter depends on background temperature, detector quantum efficiency, as well as on the emissivity of the thermal source to be upconverted.

It has long been known that all solids radiate. The power that a solid radiates is strongly dependent on its temperature and is given by Planck's formula [17]

$$\frac{dI}{d\Omega d\lambda} = \frac{dP}{dA d\Omega d\lambda} = \frac{2hc^2 \quad \varepsilon_\lambda}{\lambda^5 \left[\exp \frac{hc}{\lambda kT} - 1\right]} \qquad (3\text{-}1)$$

where $\frac{dP}{dA d\Omega d\lambda}$ is the power radiated per unit area, solid angle and wavelength, c the velocity of light, h Planck's constant, k Boltzmann's constant, and T the solid's temperature in degrees Kelvin. The body's spectral emissivity, ε_λ, is the ratio of the energy radiated by a solid at temperature T to the energy radiated by a perfect radiator or so-called "blackbody". In general ε_λ will be a function of wavelength. For a solid at room temperature (300°K) the peak of the blackbody spectral distribution is near 10 microns and the power radiated per unit area, solid angle and wavelength is $9.8 \cdot 10^6$ mks. It is interesting to note that in the 8-13 micron range the total power radiated by a 1 cm^2 blackbody at room temperature is in excess of several milliwatts. Detection of thermal radiation in the 8-13 micron region by parametric techniques requires that a substantial portion of this radiated energy be upconverted to a region of the spectrum where relatively sensitive detectors exist.

We note that equation (3-1)gives the blackbody power radiated by an object, not the blackbody radiation available at an upconverter crystal. These quantities differ because finite aperture optics are unable to collect the total radiated thermal energy. Consider the upconverter to have a usable active area of A_i and a usable collection solid angle of Ω_{io} as measured at the upconverter. (See Fig. 3-1) According to the theory of geometric optics, the area of the thermal source and radiated solid angle accepted by the upconverter are related to the similar thermal source parameters Ω and A via $n_i^2 A_i \Omega_{io} \cong A\Omega$. The n_i^2 appears because Ω_{io} is measured internally to a crystal of refractive index n_i. Further, each incremental dA $d\Omega$ accepted by the upconverter is equal to a corresponding $n_i^2 dA_i d\Omega_i$, i.e.,

$$n_i^2 dA_i d\Omega_i = dA d\Omega \qquad \Omega_i \leq \Omega_{i0} \tag{3-2}$$

In section 2 it was shown that the power density of a parametric upconverter is given by

$$I_s = \frac{\eta_i}{\eta_s} |\kappa_s \ell|^2 I_i \operatorname{sinc}^2 \frac{\Delta k \ell}{2} \tag{2-11}$$

Equations (2-11) and (3-1,3-2) describe the power density output expected by a parametric upconverter operated with a thermal or blackbody input. After some algebra it is found that the incremental output of such an upconverter is given by

$$dI_s = \frac{\eta_i}{\eta_s} (\kappa_s \ell)^2 \operatorname{sinc}^2 \frac{\Delta k \ell}{2} U_I \frac{2 hc^2 \varepsilon_\lambda}{\lambda_1^5 [\exp (\frac{hc}{\lambda_i kT}) - 1]} n_i^2 d\Omega_i d\lambda_i \ . \tag{3-3}$$

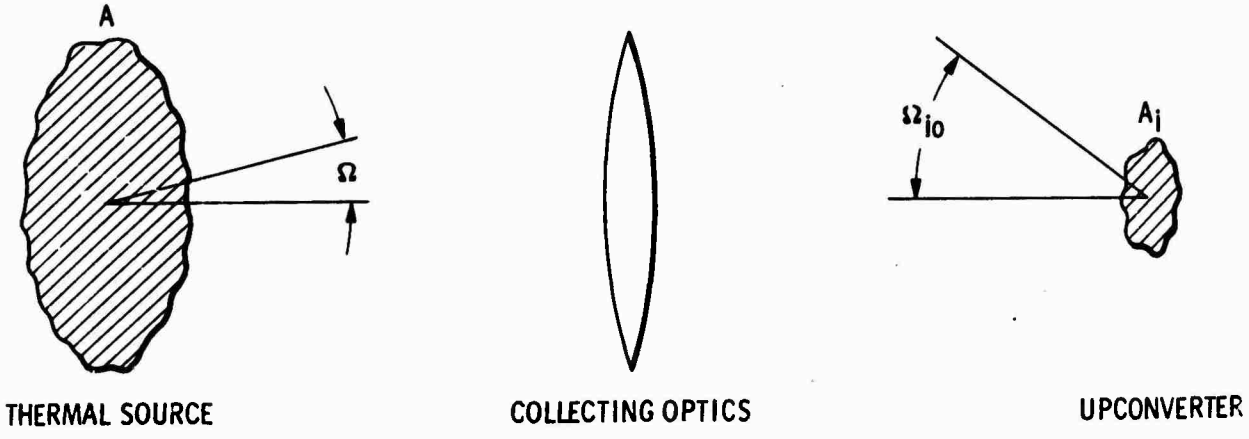

Figure 3-1 The blackbody upconverter: angular collection. Collecting optics convert a thermal source of area A, solid angle Ω into an image of area A_i, solid angle Ω_{io}.

where U_I is unity in the geometrical focal region of the thermal source, zero elsewhere (Fig. 3-2). In writing (3-3) we have implicitly assumed that there is no change in the thermal image along the length of the crystal. This assumption is equivalent to confining the crystal to the depth of field of the thermal image.

Evaluation of the total upconverter output intensity requires integration of equation (3-3) which in turn necessitates expression of the asychronism factor in terms of the angular acceptance and idler wavelength. In Fig. 3-3 we examine the phase matching condition, allowing for a small momentum mismatch, Δk. Angles are measured internally to the nonlinear crystal. It is seen that

$$\bar{k}_i + \bar{k}p = \bar{k}_s + \Delta\bar{k}$$

or

$$k_i \cos\theta + k_p \cos\phi = k_s + \Delta k$$

It is assumed that phasematching is achieved using EOO or type I phasematching so that the pump propagates as an ordinary wave through the crystal, the upconverted signal an extraordinary wave and so that the ordinary component of thermal radiation is selected for upconversion. This is the case experimentally considered in section 5 as well as that which allows the most efficient upconversion in the experimentally considered proustite - Nd:YAG upconverter. Further it is assumed that the crystal orientation angle has been chosen such that the upconverter is perfectly phase matched when the signal idler and pump are collinear. Denoting these collinear wavevectors by k_{so}, k_{io}, k_{po}, this implies

$$k_{io} + k_{po} = k_{so} \quad . \tag{3-4}$$

As ϕ is varied i.e. as the noncollinear output of the upconverter is collected the idler and signal wavelengths will vary. In addition, because the

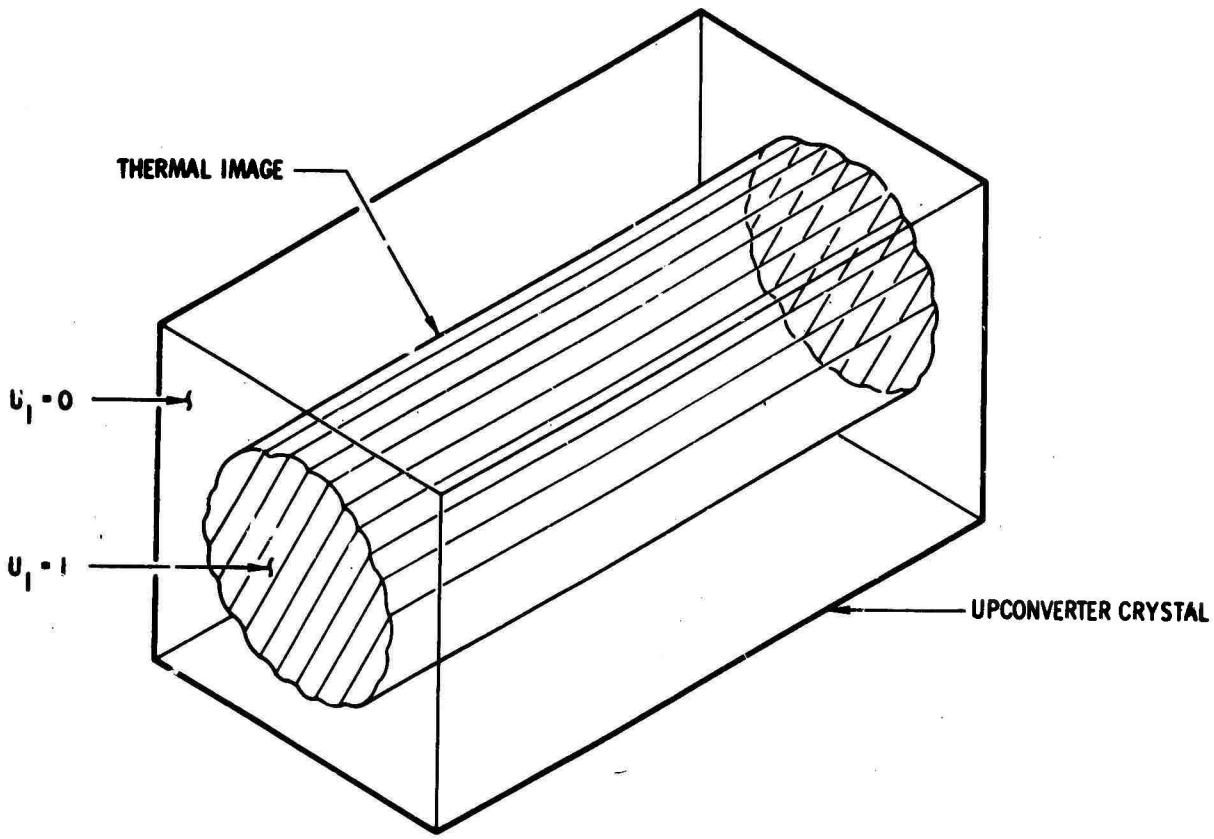

Figure 3-2 The geometric focus of a thermal scene and definition of focusing parameter U_I.

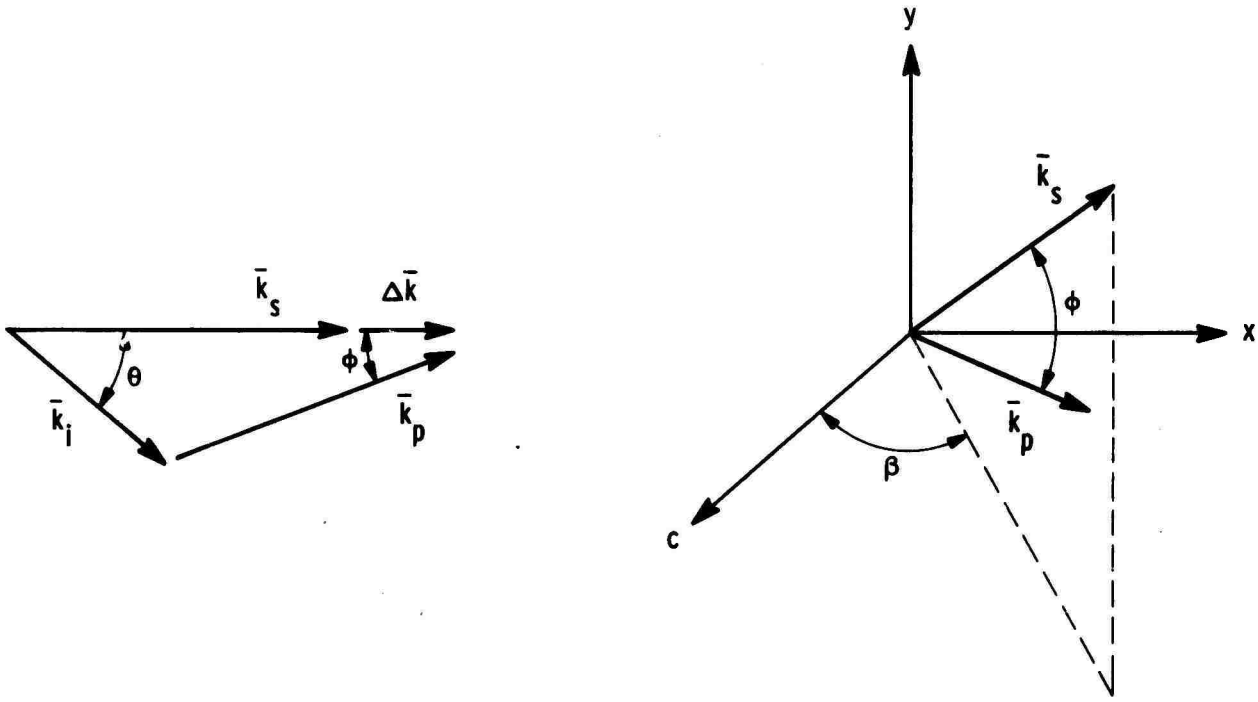

Figure 3-3 Phase matching, tuning and crystal orientation for parametric upconversion. Crystal axes are denoted by x, y and c.

signal is extraordinary, its wavevector will vary with angle. Mathematically these variations may be denoted as

$$k_1 = k_{io} + \frac{\partial k_i}{\partial \omega_i} d\omega_i \quad k_s = k \quad \frac{\partial k_s}{\partial \omega_s} d\omega_s + \frac{\partial k_s}{\partial \phi} d\phi. \tag{3-5}$$

where $d\omega$, and $d\omega_s$ denote the departure of the signal and idler radian frequencies from their collinear phase-matched values.

Using (3-3), (3-4) and (3-5), making small angle or near collinear approximations, and noting that $d\omega_i = d\omega_s$ it is found that the phase mismatch may be written

$$\Delta k = - b d\omega_i - h\phi + g\phi^2 \tag{3-6}$$

where b, h, g are defined by

$$b \equiv - \left[\frac{\partial k_i}{\partial \omega_i} - \frac{\partial k_s}{\partial \omega_s}\right] , \tag{3-7}$$

$$g \equiv \frac{k_{po} k_{so}}{k_{io}^2} , \tag{3-8}$$

and $$h(\phi) = \frac{\partial k_s}{\partial \phi} . \tag{3-9}$$

We note from figure 3-3 that in general h will be a function of the polar angle ϕ that an arbitrary upconverted ray makes with the pump as well as the angle β that the projection of that ray into the c-x plane makes with the c axis. It should be noted that the tuning of a parametric upconverter with angle can be predicted from an examination of equation (3-6) with $\Delta k=0$.

Having expressed the phase asynchronism in terms of acceptance angle and wavelength, it is possible to evaluate the total upconverted output to expected from the parametric upconverter. Using equations (3-3) and (3-6) the signal output power density is evaluated as:

$$I_s = \int_0^{\Omega_{oi}} \int_0^{\infty} F(\lambda_i T)\, U_I\, \mathrm{sinc}^2\,[-b\Delta\omega_s + g\phi^2 - h\phi]\, d\lambda_i\, d\Omega_i \qquad (3\text{-}10)$$

where Ω_{oi} is the solid angle idler acceptance of the upconverter and associated optics and where

$$F(\lambda_i,T) \equiv \frac{\eta_i}{\eta_s}\ (\kappa_s \ell)^2\ \frac{2hc^2 \varepsilon_\lambda \eta_i^{\,2}}{\lambda_i^{\,5}\ [\exp \frac{hc}{\lambda_i hT} - 1]} \qquad (3\text{-}11)$$

Observe that $F(\lambda_i T)$ closely resembles the product of a parametric gain and the Planck blackbody spectral distribution. Consider first the integration over λ_i with Ω_i fixed. Note that $F(\lambda_i T)$ is essentially constant over the range of λ_i where the sinc^2 function is appreciable. Consequently I_s may be approximated by

$$I_s \approx F[\lambda_i T)\, U_I \int_0^{\Omega_{oi}} \int_0^{\infty} \mathrm{sinc}^2\,[-b\Delta\omega_s + g\phi^2 - h\phi]\, d\lambda_i d\Omega_i \qquad (3\text{-}12)$$

Noting $d\lambda_i = \dfrac{-\lambda_i^{\,2} d\omega_i}{2\pi c} = \dfrac{+\lambda_i^{\,2} d\,[-b\Delta\omega_s]}{2\pi c b}$, I_s may be rewritten

$$I_s \approx F(\lambda_i T)\, U_I\ \frac{+\lambda_i^{\,2}}{2\pi c b} \int_0^{\Omega_{oi}} \int_0^{\infty} \sin^2\,[-b\Delta\omega_s + g\phi^2 - h\phi]\, d(-b\Delta\omega_s)\ \ d\Omega_i$$

Recall $\displaystyle\int_{-\infty}^{\infty} \frac{\sin^2 x}{x^2}\, dx = \pi.$

Hence $I_s \cong F(\lambda_i T)\, \dfrac{\lambda_i^{\,2}}{2cb}\ \Omega_{oi}$.

Collecting constants from equations (2-6) and (3-12) we find that the power density output from a blackbody parametric upconverter is given by

$$I_s = \left[\frac{\eta_o^3 \omega_s^2 \frac{d^2}{2} \ell^2 I_p}{n_s n_i n_p}\right] \left[\frac{2hc^2 \varepsilon_\lambda U_I}{\lambda^5 \exp\left[\frac{hc}{\lambda_1 kT} - 1\right]}\right] \therefore \left[\frac{\lambda^2}{cb\ell}\right] \left[n_i^2 \Omega_{oi}\right] \qquad (3\text{-}13)$$

where I_p is the pump field intensity. Each of the bracketed terms in equation (3-13) can be identified physically, i.e., I_s may be viewed as

I_s = [Parametric gain] [Blackbody density].

[Effective Spectral Bandwidth] . [Blackbody Solid Angular Acceptance]. (3-1

The equivalent spectral bandwidth for the parametric upconverter is thus seen to be $\frac{2\lambda_i}{cb\ell}$.

It is easily shown that for small angles that the blackbody solid angular acceptance of the upconverter cyrstal related to the output signal solid angular acceptance

$$\Omega_{oi} = \pi \left(\frac{k_s}{k_i}\right)^2 \frac{\phi_{ex}^2}{n_s^2} \qquad (3\text{-}15$$

where ϕ_{ex} is the angle between the signal and pump as measured externally to the upconverter crystal. In a laboratory experiment it is the choice of signal collection angle ϕ_{ex} which determines the output of the upconverter. The predicted signal output power increases as the square of the output angular aperture until the entire input Ω_{oi} is utilized.

3.2 Some Numerical Examples

We consider here two blackbody upconverter systems. The first, consisting of a proustite crystal pumped by the 1.06 micron output of a Nd:YAG laser, represents a system that has received some experimental attention as described in section 5 of this report. The second system consisting of $ZnGeP_2$ pumped by Nd:YAG,

although potentially more useful has not to date been experimentally investigated due to the unavailability of high optical quality, transparent $ZnGeP_2$.[11] The parameters necessary to calculate the upconverted power output from each upconverter are given in table I. For the proustite upconverter we note that two phase matching configurations are available, Type I or EOO and Type II or EEO.[32] Only the more efficient process, which for proustite is Type I phasematching, is considered. The indices of $ZnGeP_2$ do not allow Type I phase matching and consequently all the data shown for $ZnGeP_2$ assumes Type II phase matching.[31]

From equation (3-13) and table I we find that the expected output power densities from the two upconverters yielding a room temperature blackbody (25°C) to be given by,

$$\begin{aligned} \text{Proustite:}\quad & I_s = 6 \cdot 10^{-9}\, I_p \ell \times \left(\text{External Blackbody Solid Angle Acceptance}\right) U_I \\ ZnGeP_2: & I_s = 5 \cdot 10^{-8}\, I_p \ell \times \left(\text{External Blackbody Solid Angle Acceptance}\right) U_I \end{aligned} \qquad (3\text{-}16)$$

where I_p is the Nd:YAG power density and U_I is defined in figure 3-2.

It is interesting to calculate the power output to be expected from these upconverters. The maximum output power achievable from both upconverters occurs when U_I=1 over the non zero range of the pump. Optics may be chosen such that the pump area is smaller than the thermal image at the upconverter so that the output power will be maximized. Crystal lengths of 1 cm of proustite are presently available and although similar lengths of $ZnGeP_2$ cannot presently be acquired[11] it does not seem overly optimistic to expect such crystal lengths to be available in the future.

Further, it is reasonable to consider angular acceptances of 0.1 radian or 3.14x10-2 str and thermal emissivities near unity. Using these parameters we find the expected output from the two upconverters viewing room temperature blackbodies to be given by

$$\text{Proustite:}\quad Ps = 1.9 \cdot 10^{-12}\ P_p \text{ watts}$$

Table 1

UPCONVERTER MATERIAL PROPERTIES[11,18,24]

Property	Proustite (Ag_3AsS_3)	$ZnGeP_2$
Effective Nonlinear Coefficient, d	$2.7 \cdot 10^{-22}$ mks	$9.8 \cdot 10^{-22}$ mks
Bandwidth Parameter b	$9.3 \cdot 10^{-10}$	$9.0 \cdot 10^{-10}$
Refractive Index n_s	2.8	3.2
Refractive Index n_i	2.7	3.1
Refractive Index n_p	2.8	3.3

$ZnGeP_2$ $\quad P_s = 1.5 \cdot 10^{-11} \quad P_p$ Watts

Of course, these power outputs have a strong dependence on the temperature of the object being viewed. This temperature variation follows Planck's law (Equation(3-1) and will be further discussed later in this section. Experimental confirmation of equation 26 will be given in section 5.

3.3 Angular Acceptance and Chromatic Abberation

In the preceding sections theoretical expressions for the expected power density output from a blackbody upconverter were developed. To numerically evaluate the useful power output from a thermal upconverter, we must answer the following questions. What is the optimum acceptance aperture? What is the optimum placement and orientation of the system components?

The practical difficulty with most previously reported image upconversion experiments is that they all have relied on unique correspondence between the angles of the incoming and upconverted wave vectors with respect to the pump beam direction. As illustrated in Figure 3-4, the wave-vector conservation requirement dictates that the ratio between these two angles should be approximately the ratio of the two wavelengths.

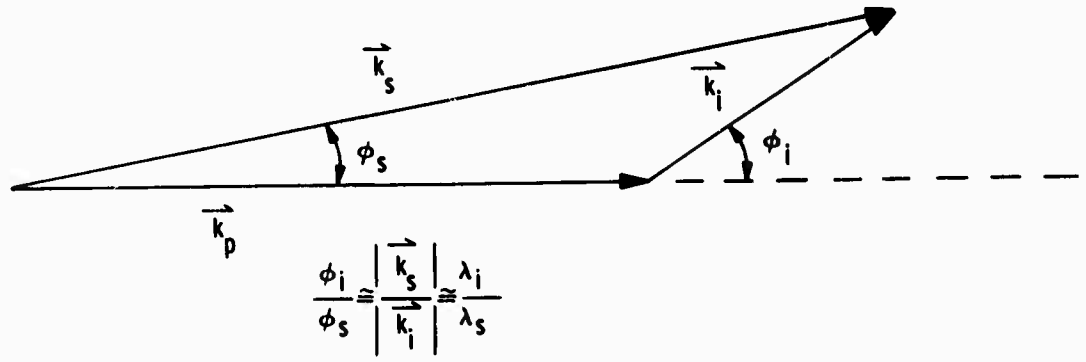

Figure 3-4 Angle Correspondence Between Infrared Input and Upconverted Output

Infrared waves of more than one frequency, but propagating in the same direction, give rise to multiple propagation directions as well as frequencies in the upconverted output (Figure 3-5). This leads to severe chromatic aberration in the upconverted image. This will be the case for all blackbody upconverters whose resolution depends on the forementioned angle correspondence.

The angle correspondence principle and chromatic aberration can be eliminated if the infrared image of the blackbody source is focused directly in the nonlinear crystal. At the focus, the image is defined by resolution elements, and not by angular resolution. Upconverted light emerging from the focused image can then be refocused to form the upconverted image, regardless of the angle at which it emerges. Hence if the depth of field of the image closely matches the length of the nonlinear crystal the individual resolution elements of the image are well defined throughout the length of the crystal. This relationship holds true not only for the oncoming infrared wavelengths but for the emerging upconverted radiation as well. Because all resolution elements are well defined throughout the crystal, they can be reimaged to form a clear visible upconverted image.

The upconversion of a single resolution element by this method is schematically illustrated in Figure 3-6. The upconversion of each of the other resolution elements proceeds independently in the identical manner.

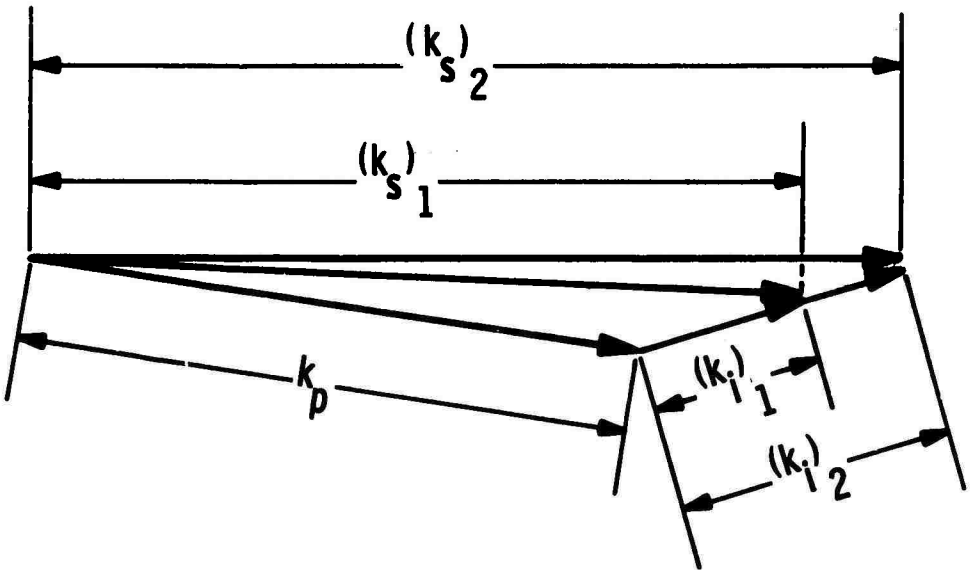

Figure 3-5 Chromatic aberration in noncollinear parametric frequency conversion.

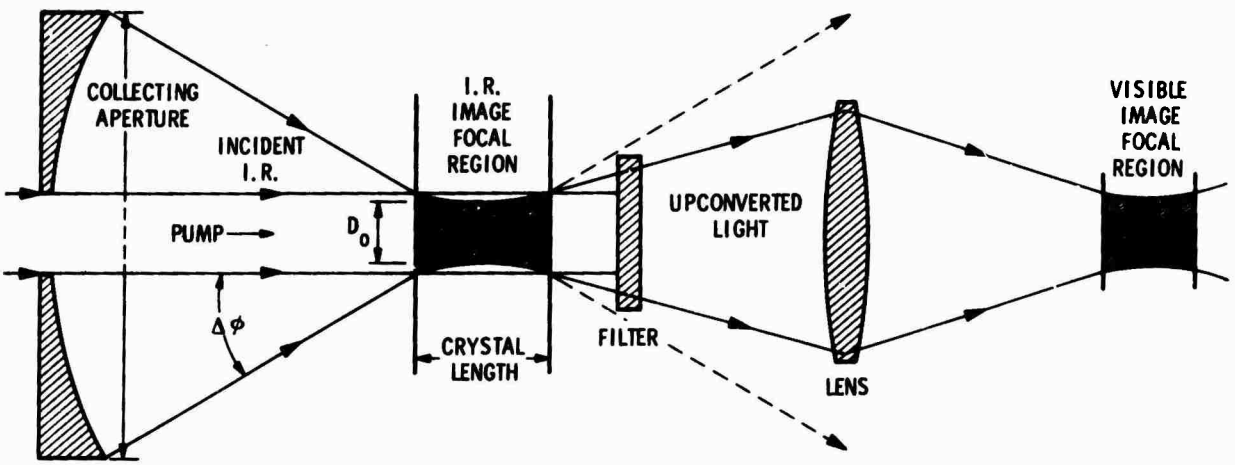

Figure 3-6. Upconversion of Single Resolution Element of Focused Image

The necessity of ensuring that the depth of field of the image is as long as the crystal length implies that the maximum usable solid angle of the blackbody radiation is given by $n_i^2 \Omega_{oi} = \frac{4 n_i \lambda_i}{\ell}$. (3-17)

If we upconvert a thermal image using the maximum allowable solid angle of $\frac{4 n_i \lambda_i}{\ell}$ we find that the signal output intensity is given by

$$I_s = \left[\frac{\eta_o^3 \omega_s^2 d^2 \ell^2 I_p}{2 n_i n_s n_p}\right] \cdot \left[\frac{2hc^2 U_\lambda}{\lambda^5 (\exp \frac{hc}{\lambda_i kT} - 1)}\right] \frac{\lambda_i^2}{cb\ell} \frac{4 n_i \lambda_i}{\ell} \quad (3\text{-}18)$$

and is independent of the length of the nonlinear crystal. Collection of blackbody radiation having a solid angle given by (3-17) places a limit on the minimum f number usable for thermal energy collection. This limit is given by

$$\text{f number minimum} = \sqrt{\frac{4n_1\lambda_1}{\pi\ell}} \quad . \tag{3-19}$$

Again consider the two potential ten micron upconverter systems, proustite and $ZnGeP_2$ pumped by 1.06 micron Nd:YAG. For the proustite system (Equation 3-19) phase-matched for upconversion of a near 10 micron image a minimum f number of $1.77 \cdot 10^{-4} \sqrt{\ell}\ m^{1/2}$ is usable. Likewise the $ZnGeP_2$ upconverter is limited to a collection f number of $1.94 \cdot 10^{-4} \sqrt{\ell}\ m^{1/2}$. For a 1 cm crystal length this implies minimum f numbers of 17.7 and 19.3 for proustite and $ZnGeP_2$ respectively. To utilize f-1 optics crystal lengths no longer than about 30 microns are usable.

The signal image output calculated from equation (3-18) is maximized and the focal length of the upconverter collection system is chosen such that the image of the thermal source extends over the entire region of the pump beam. In that case $U_I = 1$ over the region of interest and the signal output is maximum. We note that for best image performance the minimum f number of the blackbody collecting system is dictated by chromatic aberration conditions, Equation (3-19), while the focal length of the collecting system is restricted by maximum power considerations. The maximum image carrying power available from the proustite and $ZnGeP_2$ image converters per watt of input pump power as a function of the temperature of the blackbody being viewed is shown in Figure 3-7.

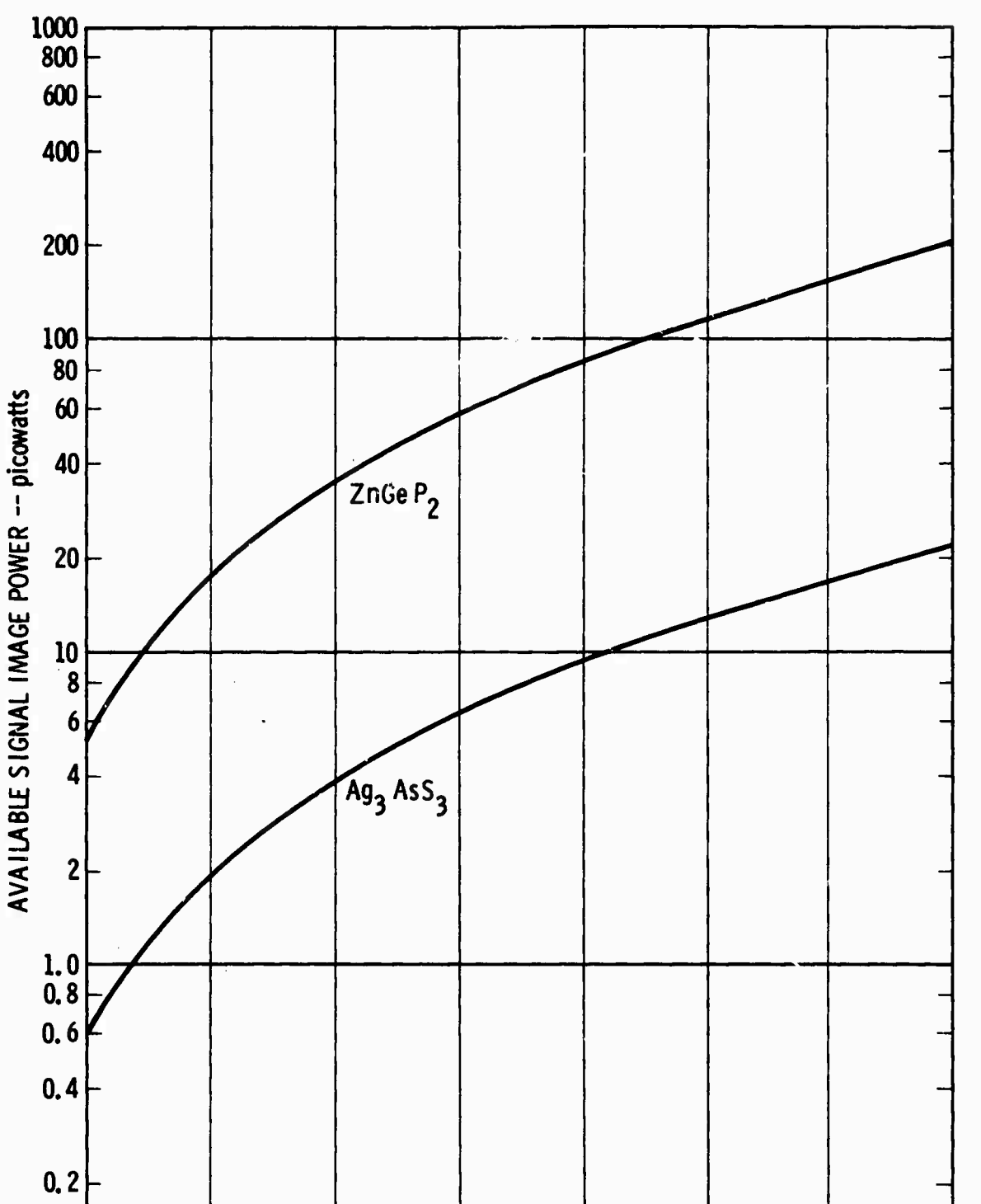

Figure 3-7. Blackbody upconversion: available signal power as a function of blackbody temperature. Pump power is assumed equal to one watt.

3.4 Resolution and Contrast

Thus far we have considered the power available in an upconverted thermal image but have said nothing about resolution to be expected from such a process. Potential resolution of the image upconverter is limited by diffraction, as well as by statistical fluctuations due to the discrete nature of light.

The least severe restriction on resolution is imposed by the minimum solid-angle-area product necessary to resolve two adjacent resolution elements. This limitation due to diffraction limits the maximum number of resolvable elements at wavelength λ_i to

$$N = \frac{A\Delta\Omega_1}{\lambda_i^2}$$

where $\Delta\Omega$, and A are the solid angle captured and the area of the detector.[19] The technique previously discussed for avoiding chromatic aberration limits the available collection solid angle to $\frac{4n_i\lambda_i}{\ell}$ where λ_i is the wavelength to be upconverted, n_i the nonlinear crystals refractive index at λ_i, and ℓ the crystal length. For a 1-cm cube proustite crystal, this means that the maximum allowed by diffraction is approximately 1000 lines or 100 ℓ/mm. For a $ZnGeP_2$ upconverter this limit increases to about 120 ℓ/mm.

Statistical fluctuations due to the low signal level are expected to place a more restrictive limit on the potential resolution of the upconverter as a thermal image viewing device. Resolution is limited by the discrete nature of the photons, and the statistical fluctuations associated with their time of arrival at the parametric upconverter. This statistical distribution of incident IR photons results

in a statistical distribution of near IR upconverted photons leaving the upconverter. In turn this results in a statistically distributed number of photons at each resolution element of any detector used to view the output of the upconverter.

In the following paragraphs we examine the limiting resolution due to so-called scintillation fluctuations in the image conversion of a near IR scene to the visible via an image tube. We will apply our results to the expermental situation where the source of the near IR image is 10 micron blackbody radiation that has been upconverted to the near IR via a proustite, or $ZnGeP_2$, Nd:YAG system.

For mathematical convenience, we will consider scene to be viewed as consisting of a pattern comprised of light and dark squares, i.e., we will consider the output of an imaging detector to be partitioned into resolution elements as sketched in Figure 3-8. We will allow for the "dark" squares to be partially illuminated and define a contrast factor C such that the rate of production of photoelectrons in elements 1 and 2 are related by

$$\dot{n}_2 = (1-C)\ \dot{n}_1 \qquad (3-20)$$

where C is always between zero and one.

The output signal may be calculated by computing the average difference in ate of photoelectron production of adjacent resolution elements. That is, an eye camera distinguishes between adjacent monochromatic resolution elements by contrasting their different levels of illumination.

Noise due to the discrete nature of photoelectrons is calculated by

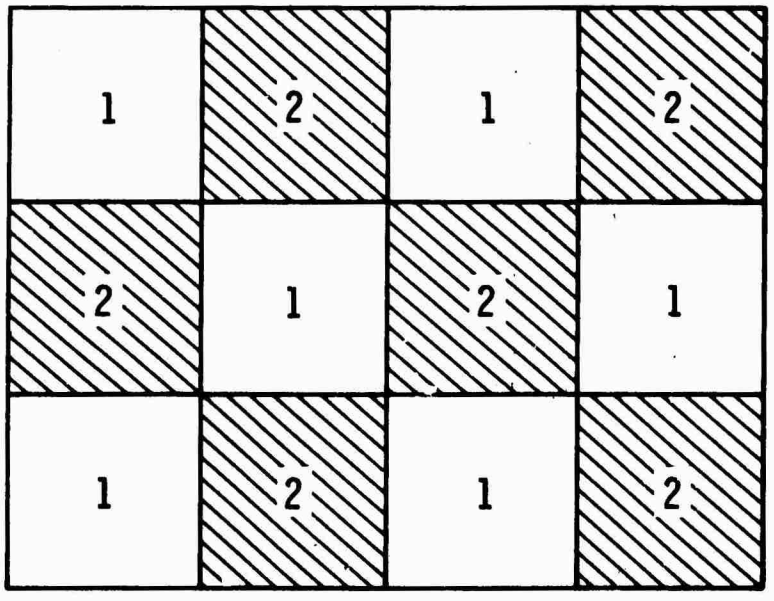

Figure 3-8 An upconverted scene. Dark squares produce (1-C) less photoelectrons than light squares.

considering the variance or rms difference in photoelectron production rates of two resolution elements. We assume as is the usual case for photon or photoelectron counting, that the production rate of photoelectrons is Poisson distributed and take the photoelectron production of adjacent resolution elements to be independent. Further, we recall that for a Poisson distribution, the average production rate is equal to the mean square rate.[19] We may write the signal to noise ratio for detection of adjacent resolution elements, i.e., the scene signal to noise ratio as:

$$\frac{S}{N} = \frac{(\bar{\dot{n}}_1 - \bar{\dot{n}}_2)\, t}{[\,(\bar{\dot{n}}_1 + \bar{\dot{n}}_2)t\,]^{1/2}} \tag{3-22}$$

where n_1 and n_2 are the average rates of production of photoelectrons in resolution elements 1 and 2 respectively. The plus sign in the denominator of the expression is due to the fact that for independent production rates mean square values add.

Noting that the total average photoelectron current is given by

$$I = \frac{Me}{2}\,[\,\bar{\dot{n}}_1 + \bar{\dot{n}}_2\,] = \frac{\eta P_s}{h\nu_s} \tag{3-23}$$

where M is the total number of resolution elements, e is the charge on an electron, η the quantum efficiency of the image detector, h Planck's constant, and ν_s the signal frequency. P_s is given by Equation (3-28) and Figure (3-7).

We may rewrite the signal to noise ratio in a useful form.

$$\frac{S}{N} = \frac{C}{2-C}\,\frac{[2It]^{1/2}}{[Me\,]^{1/2}} = \frac{C}{2-C}\left[\frac{2\eta P_s}{h\nu_s}\,\frac{t}{Me}\right]^{1/2} \tag{3-24}$$

We note that t appearing in the above equation is the integration time of the visible detector. Literature estimates of necessary signal to noise ratio for detectability, depend on the particular image, and are in the range of one to five.[20-21] For a given contract C, and a given resolution M equation (3-24) determines the minimum $(P_s)\cdot(t)$ product for satisfactory image resolution, which in turn dictates the minimum pump power-time product for image resolution.

For blackbody radiation, contrast between adjacent elements can only be due to a temperature difference between the elements. Contrast, as defined by Equation (3-20), may be determined from the Planck formula, Equation (3-1). For a scene minimum temperature of 300°K we find $C=2.07\cdot10^{-3}\ \Delta T$, where ΔT is the temperature difference between adjacent elements.

With all variables in the resolution equation (3-24) known the minimum P_{pump}-time product may be calculated.

Figure 3-9 shows the ΔT required for resolution of M elements for a Nd:YAG energy $P_p \cdot t$. This figure assumes that the output of the upconverter is viewed with a perfect detector. The resolution limits imposed by the upconversion process are shown. The $P_p \cdot t$ products shown in Figure 3-9 are reduced by a factor of about 9.3 if $ZnGeP_2$ is substituted for the proustite upconverter crystal.

If we consider detection of an image using a real image tube, whose quantum efficiency is less than unity, the $P_p \cdot t$ products shown in Figure(3-9)must be multiplied by $\frac{1}{\eta}$ where η is the quantum efficiency of the image tube.

For example, we consider an imaging system with 10^3 resolution elements. Taking the visible detector to be the eye, which has an integration time of

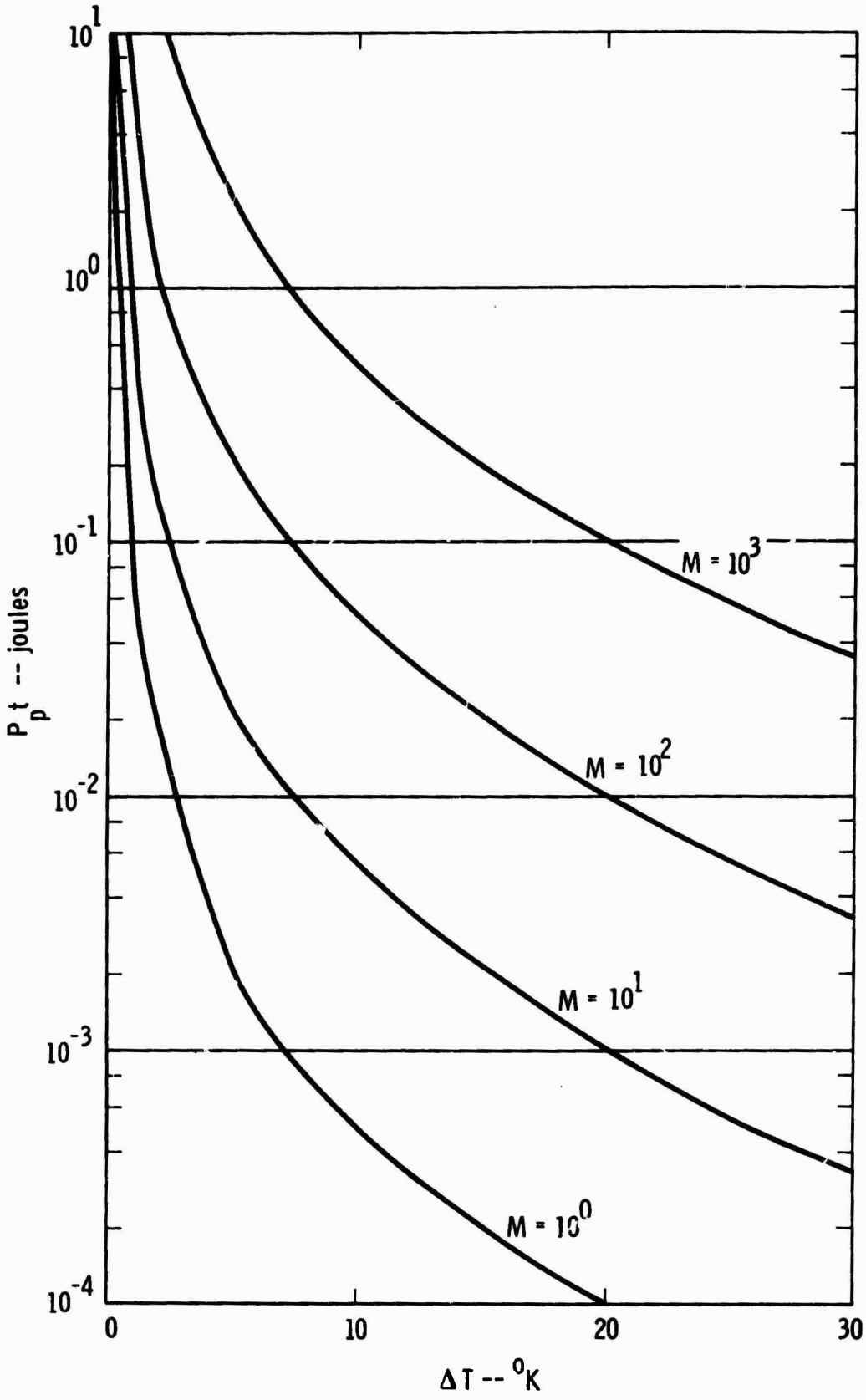

Figure 3-9 Theoretical resolution of the proustite-Nd:YAG blackbody upconverter.

approximately 0.2 seconds, considering a $\Delta T=10°K$ between adjacent resolution elements, and an InAsP photocathode image tube (see section 5) with quantum efficiency 1%, we find that the required Nd:YAG pump power for image resolution is 250 watts. Because of the damage properties of proustite, detailed in section 4 of this report, such a system is probably not presently feasible. Therefore, for detection of a 300°K blackbody image with 10^3 resolution elements it is necessary to use a detector with longer integration time than the eye (e.g. film) to develop a photosurface more sensitive in the near IR than InAsP, or to improve the damage resistance of proustite. On the other hand the construction of an upconverter using $ZnGeP_2$ with 10^3 resolution elements would require a Nd:YAG illumination of 26 watts and might be achievable.

3.5 Two Major Experimental Problems

The theory developed in the preceding parts of this report describes the power output and resolution expected from a thermal image upconverter. For viewing scenes where large temperature differences exist we expect the behavior of the thermal upconverter to approach that predicted, i.e. for high contrast thermal scenes we anticipate that the theory developed will provide an accurate description of the upconverter. For low contrast scenes (Equation(3-25))where temperature differences between adjacent resolution elements are less than several degrees, two important restrictions must be considered. First the transverse intensity variation of the pump beam must be small over the upconverter aperture. The variations across the image upconverter output should reflect variations in thermal scene temperature, not variations in pump intensity. For detection of 1°C differences from a 300°K background this implies that the pump be uniform to substantially better than 0.2%. Alternately if this uniformity is not achievable, some method must be devised for compensating for the pump induced variation in the output scene.

The second difficulty encountered in viewing a thermal scene having small temperature gradients is the low contrast of the scene itself. For room temperature background scene contrast is given by $C \tilde{=} 1.7 \cdot 10^{-3} \Delta T$.
Low scene contrasts are difficult to maintain in any device viewing the output of the thermal converter. These small contrasts imply that image tube photocathodes or film surfaces used to amplify or record the upconverter image output must be uniform to within less than a fraction of one per cent. This requirement is presently impossible to satisfy. It is expected that it will be necessary to employ some artifical means of image contrast enhancement before the thermal image upconverter can be successfully used to view a low contrast thermal scene. Image contrast enhancement will not only relax requirements for detector uniformity but will also allow presentation of an upconverted thermal image with an improved signal to background ratio.

Section 4

EXPERIMENTAL EFFORTS: UPCONVERSION OF A COHERENT SOURCE

4.1 PROUSTITE : MATERIAL PROPERTIES

Proustite, known for many years as naturally occurring crystal, was first artificially synthesized in 1966 at the Royal Radar Establishment in England[18]. Beginning with the work reported by Hulme and others in 1967, the properties of proustite have been the subject of several experimental investigations. Proustite has been used for frequency doubling of the CO_2 laser,[22] for upconversion[23] of CO_2 as well as for parametric oscillation.[24]

Crystalline proustite belongs to crystal space group $R3_c$ and is transparent from 6000Å to 13 microns. Although the optical quality of presently available crystals is good, scattering centers are visible in all samples we have examined to date. A typical piece of proustite, grown at the Royal Radar Establishment in the United Kingdom, is shown in Figure 4-1.

Proustite's second order nonlinear coefficients, among the largest of all synthetically produced crystals, are greater than twice those of lithium niobate.[18] In spite of proustite's large nonlinearity, its usefulness for nonlinear optics is limited by its lack of resistance to damage by intense laser light.

We have observed a 5 watt, unfocused, multimode cw Nd:YAG laser cut in half a thin polished piece of proustite (see Figure 4-2). Further, we observe that a repetitively Q-switched Nd:YAG laser with a peak density of 500 kW/cm^2 causes pitting of a polished proustite sample. These damage

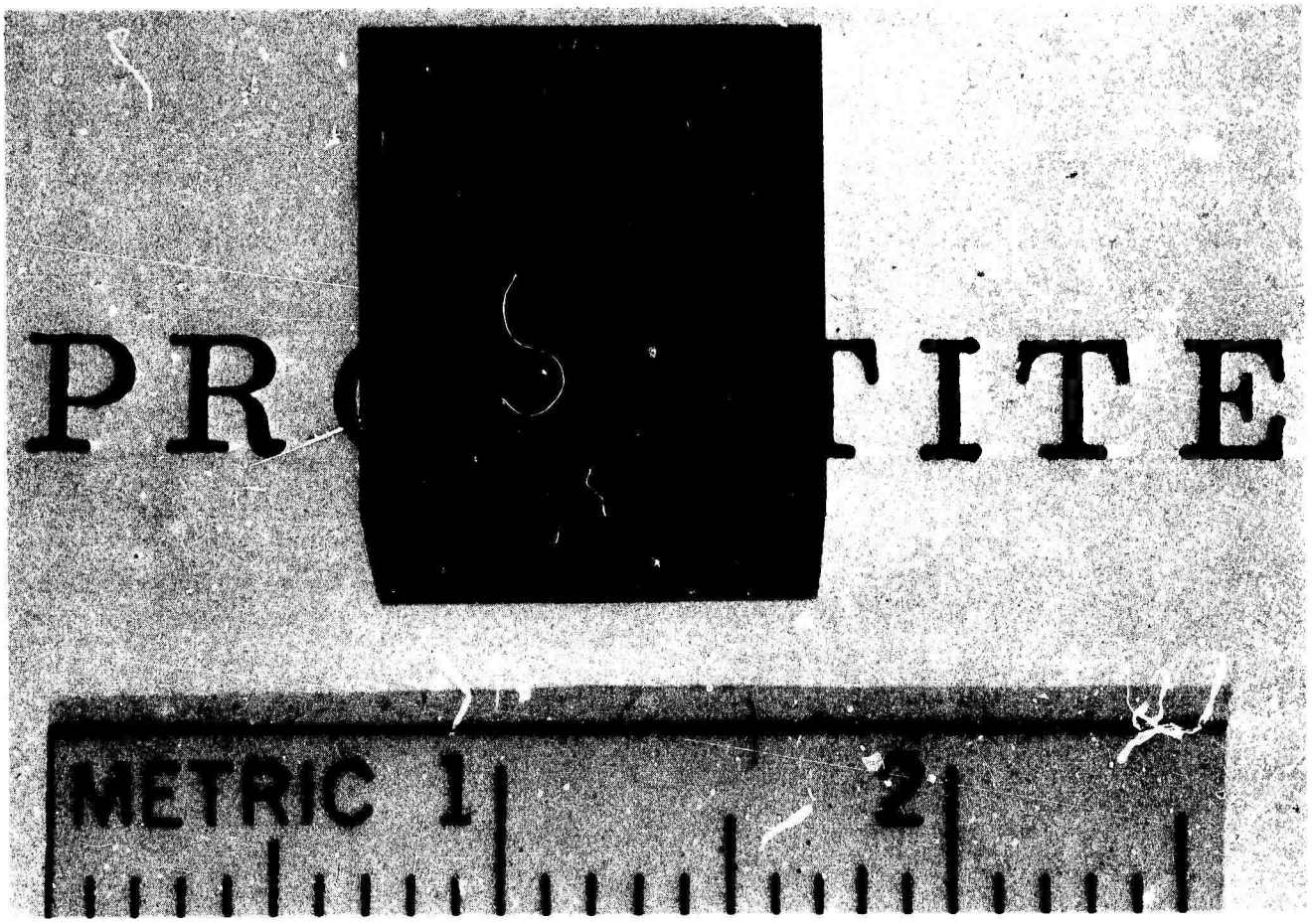

Figure 4-1 A proustite cube, as received from the Royal Radar Establishment, United Kingdom.

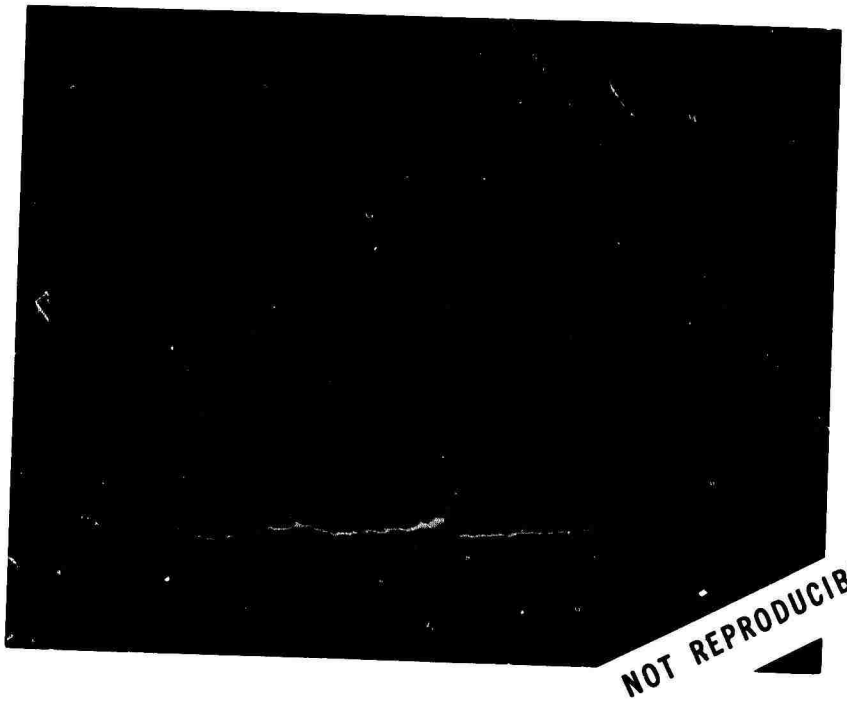

Figure 4-2 Damage to a thin slab of proustite.

The proustite cracked into two pieces as a result of the heating due to a 3 watt multimode Nd:YAG laser. Photo magnification is approximately 15.

thresholds are at least on order of magnitude worse than those previously reported.[25]

At Nd:YAG illumination power densities just below those necessary to permanently damage the proustite we found that the temperature of the proustite crystal was raised to a point where it was hot to the touch. Such heating indicates significant absorption at 1.06 microns. Because of the large change in proustite's temperature with low power Nd:YAG illumination it is of interest to consider how the bandedge of proustite varies with temperature. We have made transmission measurements on a 1 cm x 1 cm x 1 cm proustite cube at temperatures of 30°C, 50°C, 100°C, 150°C, 200°C, and 250°C using a Cary 14 spectrophotometer. The results of these measurements are shown in Figure 4-3, where crystal transmission (for the ordinary ray) is plotted versus wavelength for several different values of temperature. From Figure 4-3 it can be seen that the bandedge of proustite shifts towards longer wavelengths as temperature is increased. In going from 30°C to 250°C, the total bandedge shift is approximately 850Å.

Let us suppose now that at room temperature, there is some residual 1.06 micron absorption due to the tail of the bandedge. If this absorption causes heating of the crystal, the bandedge will be shifted into a region of still higher absorption. This in turn can cause still more heating, with further temperature rise, and so forth. This then is, in effect, a thermal runaway process which could result in melting of the crystal. To avoid this possibility, it is desirable to choose the proustite phasematching angle so that the required phasematching temperature is as low as possible. Cooling of the crystal might even prove desirable in some circumstances. In any case,

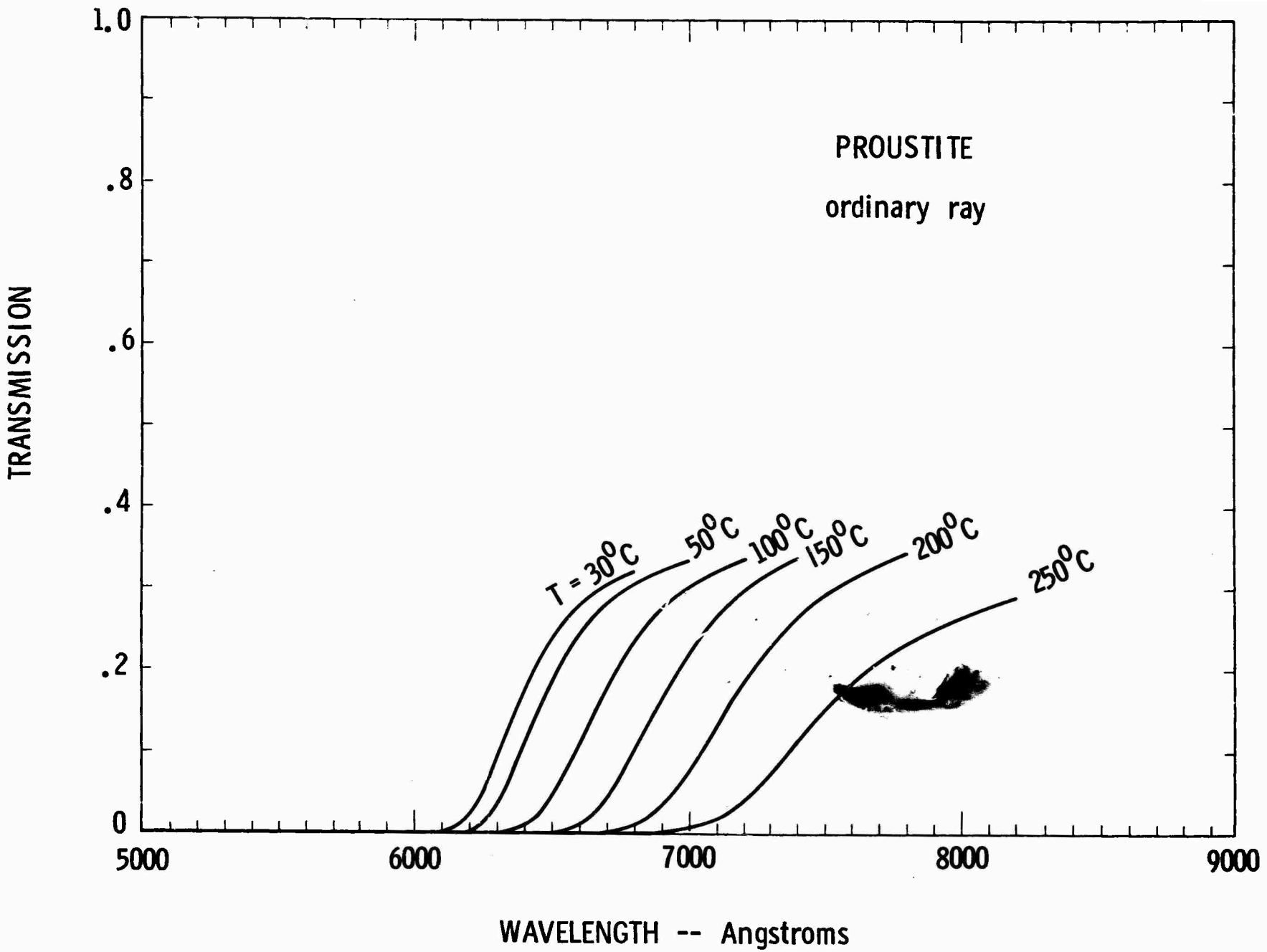

Figure 4-3 Bandedge dependence upon temperature for the ordinary ray in proustite.

it is clear that high phase-matching temperature should be avoided in operation of a proustite upconverter. All experimental efforts described in this report used proustite oriented for room temperature phasematching.

4.2 UPCONVERSION IN PROUSTITE:THEORY

Two different orientations are possible for Nd:YAG pumped 8-13 micron upconversion in proustite. In the first configuration, termed type I or EOO phase matching, the far IR radiation propagates as an ordinary wave, the pump as an ordinary wave and the upconverted signal as an extraordinary wave. In the second, termed type II or EEO phase matching, the upconverted signal and infrared wave are extraordinary, the pump ordinary.[26]

For efficient parametric upconversion the familiar conservation of momentum and energy relations must be satisfied, i.e.,

$$\omega_{pump} + \omega_{far\ IR} = \omega_{signal} \tag{4-1}$$

$$\bar{k}_{pump} + \bar{k}_{far\ IR} = \bar{k}_{signal} \tag{4-2}$$

where $\omega_{far\ IR}$, the far IR frequency is to be upconverted to ω_{sig} the signal frequency. For a Nd:YAG pumped, 8-13μ, upconverter these relationships can be satisfied with a proustite crystal cut with its length close to 20 degrees from the crystalline optic axis. The exact "phase matching" angle is dependent on whether type I or type II phase matching is used and is easily determined experimentally.[26]

As shown in Section 2 of this report the upconversion efficiency of a parametric upconverter is proportional to the square of the relevant nonlinear coefficient and is different for type I and type II phase matching.

It is easily shown that the effective nonlinear coefficient for type I phase matching is given by

$$d_{eff} = d_{31} \sin\theta - d_{22} \cos\theta \sin 3\phi, \tag{4-3a}$$

while for type II matching

$$d_{eff} = d_{22} \cos^2\theta \cos 3\phi \tag{4-3b}$$

where θ and ϕ are the angles the crystal z and x axes respectively make with the crystal length.[27] Noting, that for proustite, $|d_{22}| = 1.6\,|d_{31}| = 2.3 \cdot 10^{22}$ mks[18] and recalling that $\theta = 20$ degrees[26] is required for phase matching, the effective nonlinear coefficients may be maximized by appropriate choice of ϕ. For type I phase matching, the effective nonlinear coefficient is maximized by choice of $\phi = +90$ degrees and is given by

$$d_{\text{effective maximum}} = 1.84\, d_{31} = 2.66 \cdot 10^{22} \text{ mks},$$

while for type II phase matching, $d_{\text{effective maximum}}$ is achieved with $\phi = 0$ and is given by

$$d_{\text{effective maximum}} = 1.39\, d_{31} = 2 \cdot 10^{-22} \text{ mks}.$$

Hence, the type I upconverter can be designed to utilize a nonlinear coefficient 1.33 times that of the maximum possible with type II phase matching.

For the type I phase matched upconversion of a Gaussian laser beam, an exact theoretical analysis exists. This analysis, in contrast to the

approximate treatment given in Section 2 takes into account the effects of losses, double refraction and arbitrary focusing. The theoretical predictions for the EOO-type I, proustite, Nd:YAG pumped, 10.6 micron upconverter are summarized below. For a complete description of the arguments that lead to the equation below the reader is referred to papers by Boyd and Kleinman.[28,29]

Briefly, Boyd and Kleinman's results predict that the power output of such a 10.6 micron upconverter is given by

$$\frac{P_s}{P_{10.6 \text{ microns}}} = 1.42 \cdot 10^{-9} P_p \ell h(\beta, \xi) \text{ cgs} \qquad (4\text{-}4)$$

where $\beta = 12.5 \ell^{1/2}$

where P_s, $P_{10.6}$, P_p are the powers of the 0.967 micron wavelength signal, the 10.6 micron radiation and 1.06 micron Nd:YAG laser, respectively. ℓ is the crystal length, ξ the focusing parameter of the Nd:YAG and CO_2 beams, β is a walkoff parameter and $h(\beta, \xi)$ which describes the effects of focusing, is given from the graph of Figure 4-4.

For a one centimeter length piece on proustite, with loosely focused CO_2 and Nd:YAG beams, ($\xi = 10^{-2}$) Equation(4-4)predicts an upconverted power of approximately $10^{-4} P_{10.6} P_p$. For example, for 100 mW of CO_2 and YAG power incident upon the proustite we would expect roughly 10^{-6} watts of upconverted signal at 0.9670 microns.

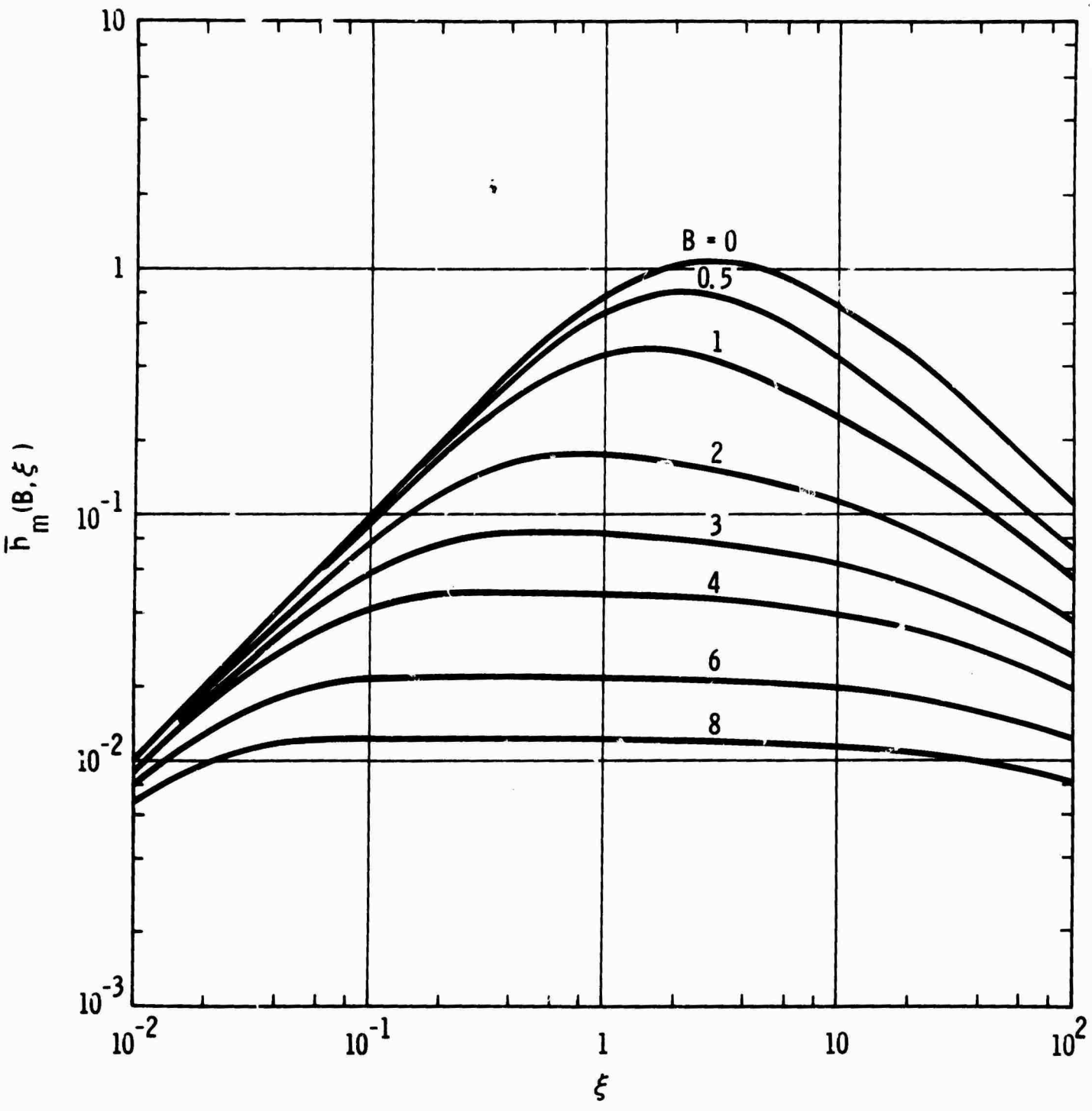

Figure 4-4 The effects of focusing and double refraction in the EOO or Type I upconverter. $\xi = \ell/b$ where b is the Nd:YAG and CO_2 confocal parameter. For the proustite upconverter $\beta \quad 12.5\ (\ell)^{1/2}$.

For type II phase matching no exact analysis exists but the approximate analysis given in Section 2 of this report may be used to predict the upconverted power of a CO_2, Nd:YAG mixing experiment. This approach neglects walkoff and diffraction, but should, in general, give reliable predictions of upconverted power if the nonlinear crystal lies in the near field region of loosely focused Nd:YAG and CO_2 laser beams.

Subject to these assumptions, the power output of a type II phase matched CO_2, Nd:YAG mixing experiment can be calculated from Equation (2-16) yielding

$$\frac{P_s}{P_{10.6}} = 2.4 \cdot 10^{-7} \ell^2 \frac{P_p}{A_p + A_i},$$

where A_p and A_i are the areas of the Nd:YAG and CO_2 beams and it is assumed that both beams are lowest order transverse modes of their respective laser cavities.

For parameters identical to those considered for type I phase matching

$$\frac{P_s}{P_{10.6}} = 1.2 \cdot 10^{-5} P_p$$

or for $P_p = P_{10.6} = 0.1$ watts

$P_s = 1.2 \cdot 10^{-7}$ watts, or less than 1/8 that for type I phase matching.

4.3 UPCONVERSION IN PROUSTITE : EXPERIMENT

As a partial experimental verification of the theory presented in the preceeding sections of this report, the output of a CO_2 laser operating

at several wavelengths near 10 microns was upconverted to a wavelength near 0.95 microns by mixing it with the 1.06 micron line from a Nd:YAG laser.

Mixing was initially accomplished in proustite using type II or EEO phase matching. Although type I phase matching provides better upconversion efficiency and is better theoretically understood, the availability of a crystal oriented for type II phase matching led us to begin our upconversion study with an experimental investigation of type II mixing. For our initial type II mixing experiments, upconversion was accomplished with the CO_2 laser operating at 9.6 microns, 10.2 microns and 10.6 microns. The particular wavelength CO_2 wavelength to be upconverted was selected by rotation of the proustite crystal. Subsequent experimentation utilized a CO_2 laser partially filled with SF_6 to suppress oscillation in all but the 10.6 micron CO_2 line. Single line operation of the CO_2 laser by this method was only partially successful and the laser often oscillated in two spectral lines near ten microns.

The angular acceptance of the upconversion process was measured yielding a value close to that previously reported in the literature.[27]

Upconversion was achieved with the Nd:YAG laser operating in both cw and Q-switched modes. Typical cw Nd:YAG powers incident on the proustite crystal were 50-300 mW while average CO_2 powers were 50-150 mW. When the Nd:YAG laser was Q-switched, the average power was 200 mW, with peak powers of 500 watts. As expected, Q-switching the Nd:YAG laser significantly increased the peak power of the upconverted signal, while reducing the

possibility of damage to the proustite crystal by limiting the average power incident upon it.

Experimentation with focusing of the Nd:YAG laser as well as the CO_2 laser was undertaken. Lenses of focal lengths 75 cm and 10 cm were used for the CO_2, lenses of 50 cm and 25 cm focal lengths were used for the Nd:YAG. As expected the upconverted power increased with stronger focusing and was usually strong enough to be seen with an uncooled type 7102 phototube.

Considerable effort was made to extend the minimum detectable signal to its lowest possible value. Provision was made for cooling the type 7102 photomultiplier to dry ice temperature ($-68^{o}C$). Such cooling decreased its noise equivalent power from about 10^{-13} watts at room temperature to about $3 \cdot 10^{-15}$ watts at $-68^{o}C$ (1 sec integration time). Provision was made for beam steering of both the CO_2 and YAG laser beams as well as adjusting the angle and position of the proustite crystal. A schematic diagram of the experimental setup used is shown in Figure 4.5. The CO_2 laser beam, chopped at 1 KHz was focused by a 10 cm focal length mirror upon the proustite crystal. The Nd:YAG, focused by a 25 cm lens, passed through a hole in the CO_2 mirror, and onto the proustite. The 0.967 micron output was detected using phase sensitive detection with typically one second integration time. Three bandpass filters and a polarizer prevent both the CO_2 and the YAG radiation from entering the detector. A KCl reflector and teflon attenuator provide CO_2 powers, at the proustite input face, variable from 1 microwatt to 100 milliwatts. Focusing as shown provides approximately equal CO_2 and Nd:YAG beam areas measured to be approximately $1.03 \cdot 10^{-2}$ cm^2, or CO_2 and Nd:YAG focusing parameters of approximately $3.0 \cdot 10^{-2}$ and $2.5 \cdot 10^{-1}$ respectively.[28] It might

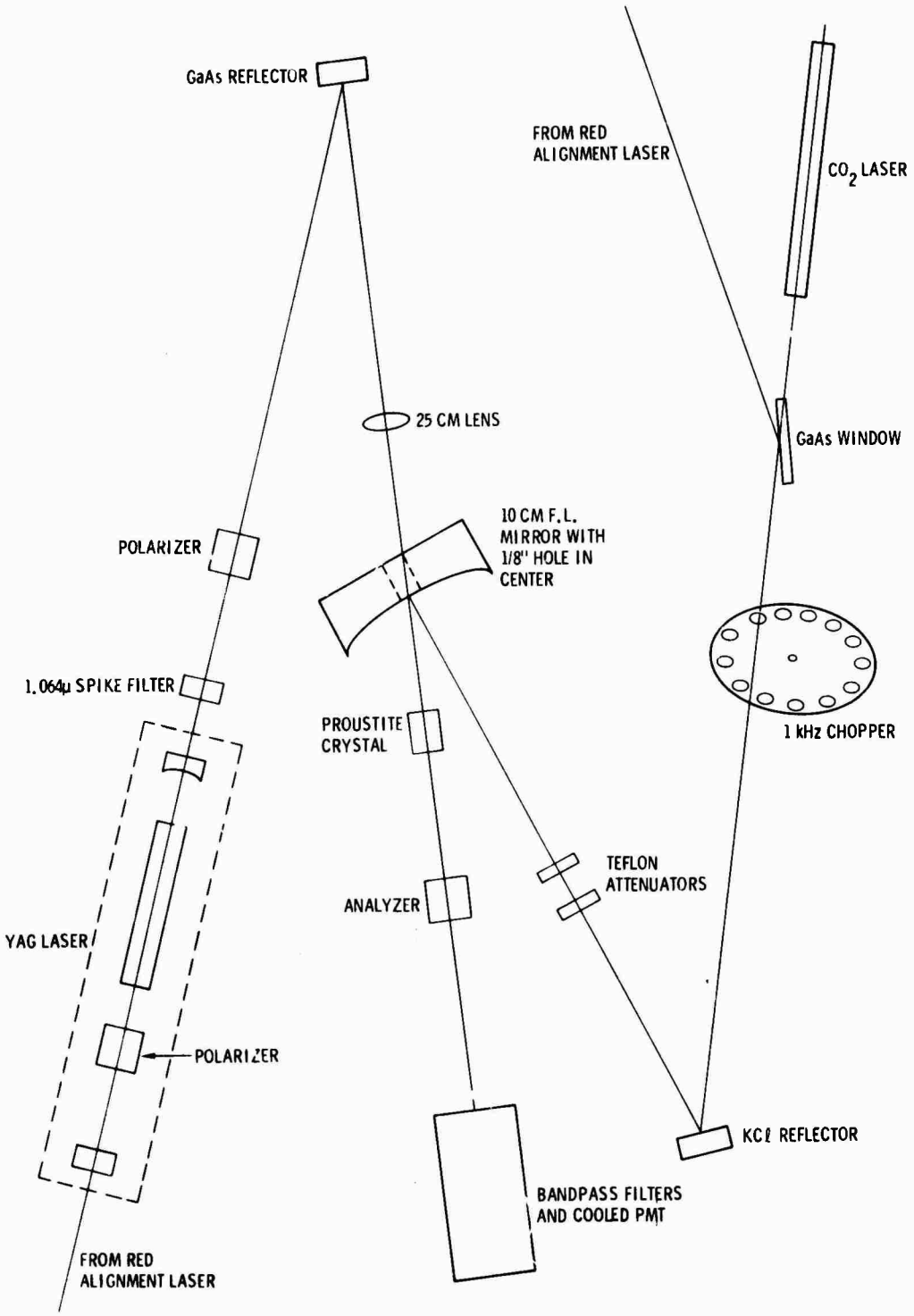

Figure 4-5 A schematic diagram of the parametric upconverter.

be desirable to focus the Nd:YAG tighter to optimize upconverted power by making the Nd:YAG focusing parameter more nearly equal to that of the CO_2 beam. This was not tried for fear of damaging the proustite at moderate (less than 50 mW) power levels with any stronger focusing.

The typical Nd:YAG pump power for the experiment shown schematically in Figure 4-5 was 60 mW. Detection of 80 milliwatts of CO_2 incident upon the proustite crystal was accomplished with a signal to noise ratio of greater than $2 \cdot 10^5$, leading to an expected minimum detectable signal power of approximately 0.5 microwatts. Detectability of about 1 microwatt of CO_2 was verified by inserting teflon attenuators in the CO_2 beam to reduce its power to the microwatt level. Figure 4-6 shows a photograph of our experimental setup. Figure 4-7 shows typical upconverter output waveforms.

More efficient upconversion is possible using type I phasematching. As noted earlier the nonlinear coefficient governing the mixing process is expected to be greater for type I matching than for type II matching. Type I experimentation indicates at least qualitative agreement with theory. Type I upconversion efficiencies observed in an experimental arrangement identical to that used for type II mixing were several times greater than the type II configuration.

Type I or EOO mixing was observed with both cw and Q-switched Nd:YAG pumps. In preparation for the pulsed upconversion experimentation we constructed an electrooptic Q-switch for use on the upconverter program. Pulsed upconversion allows us to detect CO_2 radiation of less than several microwatts using a cooled type 7102 S-1 detector. Continuous Type I upconversion

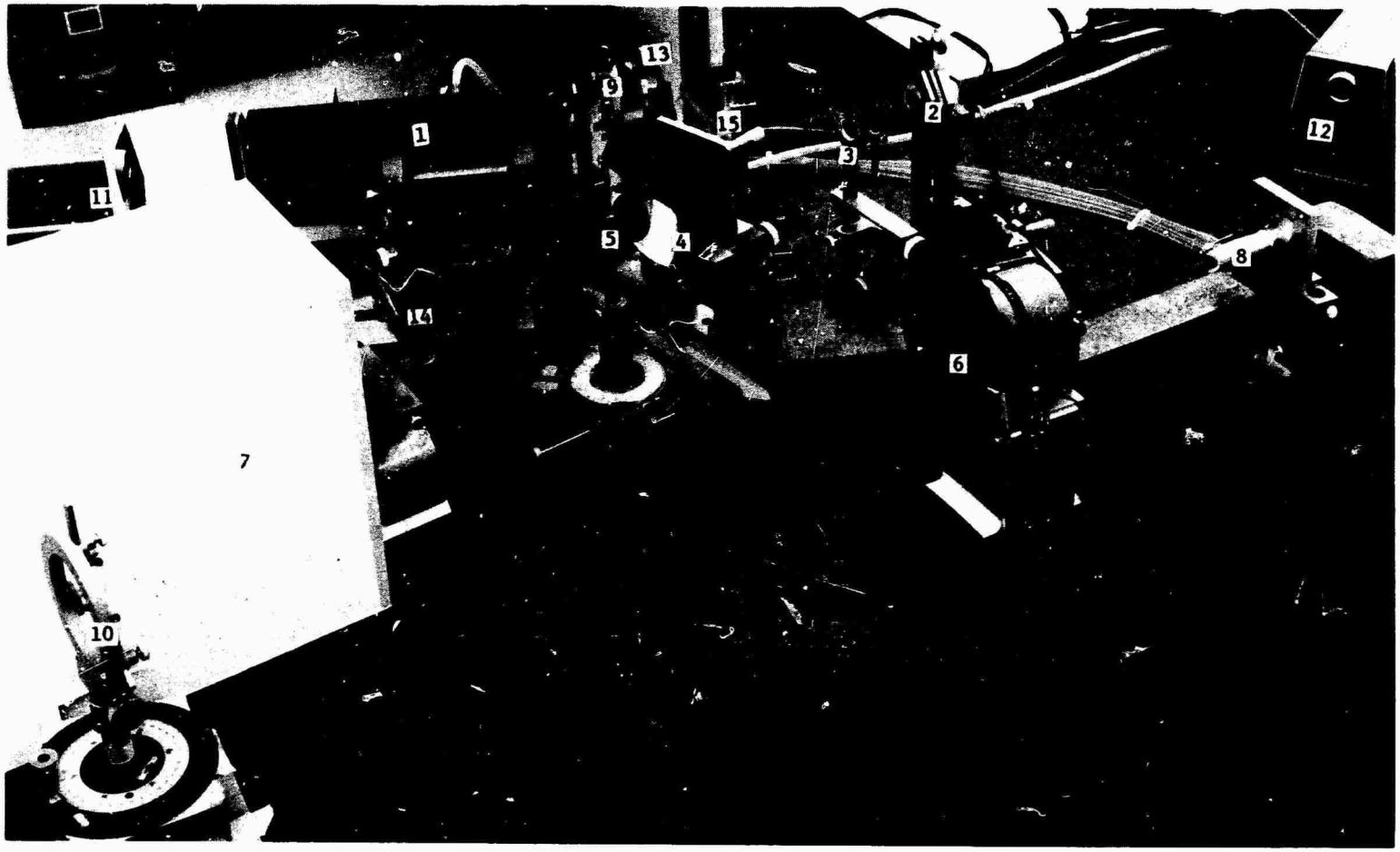

The numbers on the photograph identify the components as follows:

1. Nd:YAG laser
2. GaAs reflector
3. Nd:YAG focusing lens
4. CO_2 focusing mirror
5. Proustite crystal
6. 1 KHz chopper wheel
7. Cooled PMT and bandpass filters
8. GaAs window for CO_2
9. Nd:YAG narrow bandpass filter
10. KCl reflector
11,12. Alignment lasers
13. Polarizer
14. Analyzer
15. 3 db Nd:YAG attenuator

Figure 4-6 The Parametric Upconverter

Figure 4-7 Type II parametric upconverter output waveforms.

For this photo, the Nd:YAG laser output was chopped at a 1 KHz. CO_2 input radiation was about 10 mW, Nd:YAG radiation about 100 mW. Upper trace is upconverted signal, lower trace is the Nd:YAG waveform. The signal power is of the order of several nanowatts.

performed, using phase sensitive detection, was limited by detector dark current. Minimum CO_2 powers of several microwatts were easily detected. Pulsed upconversion has the advantage that the output of the detector used may be gated in synchronism with the pump such that the effective dark current of the detector is reduced by the duty cycle of the gating. We note that the pulsed techniques used to upconvert a point CO_2 source are applicable to image upconversion, whereas phase sensitive detection, used in the cw mixing experiments, is not adaptable to image upconversion.

Section 5

EXPERIMENTAL EFFORTS : UPCONVERSION OF A THERMAL SOURCE

5.1 INTRODUCTION

In Sections 2 and 3 of this report the theory of a black body upconverter was developed. These numerical predictions were made for the output from both a proustite-Nd:YAG and a $ZnGeP_2$-Nd:YAG upconverter. Calculations were made for arbitrary thermal radiation angular acceptances as well as for angular acceptances intentionally limited to avoid chromatic abberation. In this section experimental efforts aimed toward detecting the output of both imaging and non-imaging thermal upconverters are described. Because proustite is commercially available and $ZnGeP_2$ is not only the proustite-Nd:YAG upconverter was experimentally investigated. The output of the non-imaging proustite upconverter was successfully observed with a phototube. Attempts at viewing the upconverted signal with an image tube were, however, unsuccessful. Efforts at detection of an upconverted thermal image failed because of: 1) The poor resistance of proustite to damage by Nd:YAG radiation, 2) the inadequate performance of the image tube used to view the upconverter output.

5.2 THE NON-IMAGING UPCONVERTER-PHOTOTUBE DETECTION

The non-imaging upconverter described here detects thermal radiation in the 6-13 micron spectral region. Upconversion is accomplished in proustite by mixing the thermal radiation with the 1.06 micron output of a Nd:YAG laser.

Figure 5-1 shows a schematic diagram of the upconverter. The blackbody radiation is produced by either a heated aluminum plate or by a commercial blackbody source and is collected by a 6 cm focal length spherical mirror arranged so that its numerical aperture is 0.125.

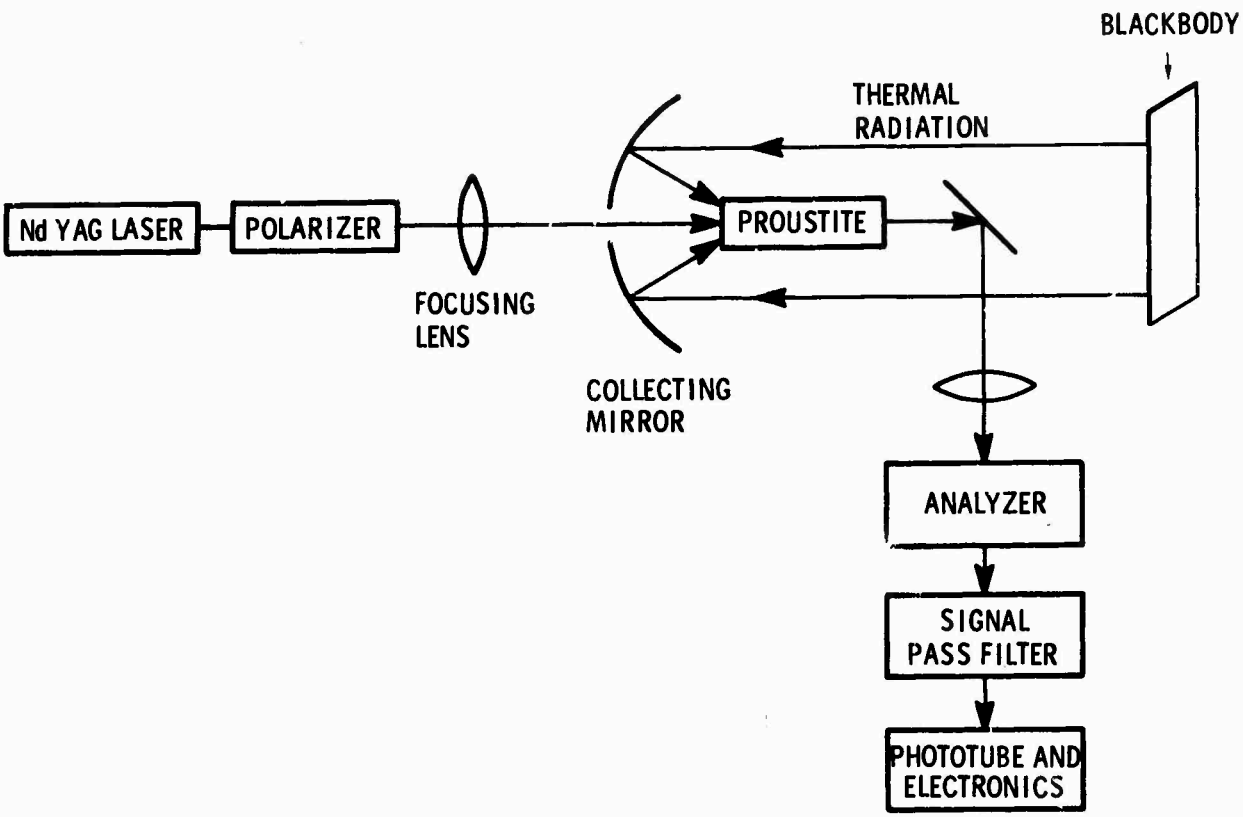

Figure 5-1 The blackbody upconverter: a schematic diagram. The output of the upconverter was collected by a 15-cm focal-length lens.

The Nd:YAG pump laser is continuously pumped and repetitively Q-switched and produces peak powers of 1 kW with prf of 2 kHz and average power of 100 mW. The output of the laser is passed through a 1/8" diameter hole in the blackbody collecting mirror and is focused by a 25 cm lens into the proustite crystal. The upconverted signal, whose wavelength is near 9.5 microns, is observed with a S-1 surface photomultiplier (ITT FW-118) cooled to dry ice temperature ($-68^{\circ}C$). Electronics are provided for photoelectron counting. Figure 5-2 shows a photograph of the experimental arrangement.

Upconversion is accomplished using type II phase-matching in a 0.6 cm long piece of proustite oriented with its length $20^{\circ} \pm 1^{\circ}$ from the crystallographic "c" axis. The crystal is cut with its length in the yz plane so that the contributions from the d_{22} and d_{31} nonlinear coefficients to the second order polarization add. (See Equation (4-3a)).

The performance of a parametric upconverter used for detection of blackbody radiation was theoretically analyzed in Section 3 of this report. There it was found that (see Equation (3-13)) the variation in the output of the thermal upconverter is dependent solely upon the change in blackbody radiation with temperature and is given by

$$P_s = \frac{2hc^2 \varepsilon K}{\lambda_i^5 \left[\exp \frac{hc}{\lambda_i kT} - 1 \right]} \qquad (5\text{-}1)$$

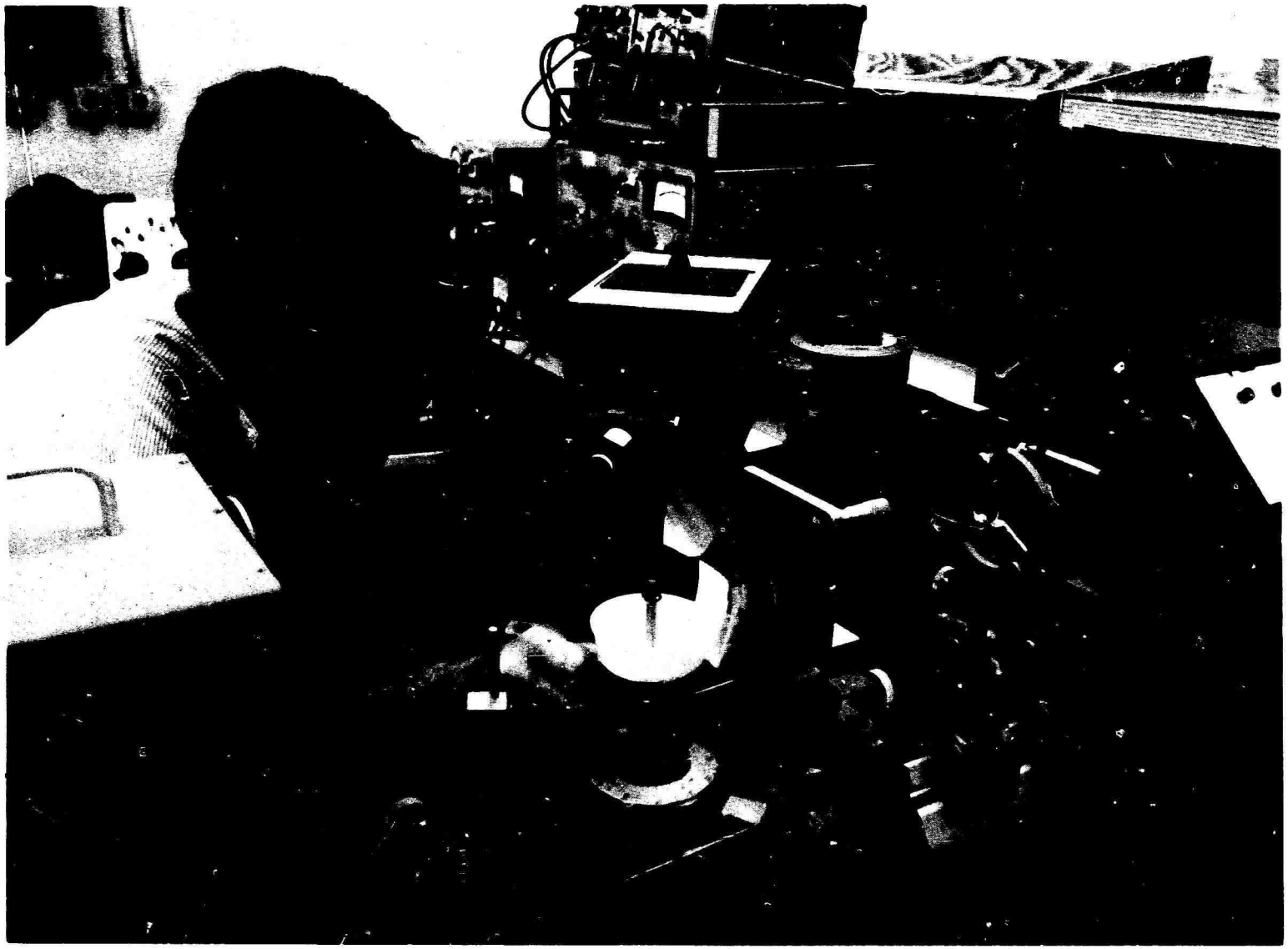

Figure 5-2 The blackbody upconverter.

where P_s is the upconverted signal power, λ_i the blackbody wavelength selected by the upconversion parametric process, c the velocity of light, h Planck's constant, k Boltzmann's constant, T the solid's temperature in degrees Kelvin, ε the emissivity of the radiating solid and K is a gain constant independent of T which totally describes the upconverter. Included in K are the effects of focusing, crystal length as well as spectral and solid angle acceptances of the parametric upconverter.

Figure 5-3 shows the measured and computed 0.95 micron upconverted output as a function of a heated solid's temperature. The upper solid line shows the output expected from the upconverter as given from (5-1) for a perfect or so-called blackbody radiator ($\varepsilon = 1$). The lower solid curve, agreeing closely with the experimentally measured variation, is computed for a solid with emissivity of 0.7. From the experimental data it is observed that the upconverter is able to "see" a 300° K object without external illumination. It should also be noted that Figure 5-3 implies that objects having temperatures only a few degrees apart have been distinguished. Much of the present ambiguity in distinguishing temperatures less than a few degrees apart is traceable to temporal instabilities in the output of the Nd:YAG laser. With development the parametric upconverter should be able to discriminate between objects different in temperature by a fraction of a degree.

The wavelength parametrically upconverted is selected by rotation of the proustite crystal. Figure(5-4)shows the IR wavelength upconverted as a function of the angle between the Nd:YAG pump and the crystal length. The upconverted signal wavelength was measured with a 1/2 meter Jarrell-Ash grating spectrometer, and the far infrared wavelength plotted in Figure 5-4

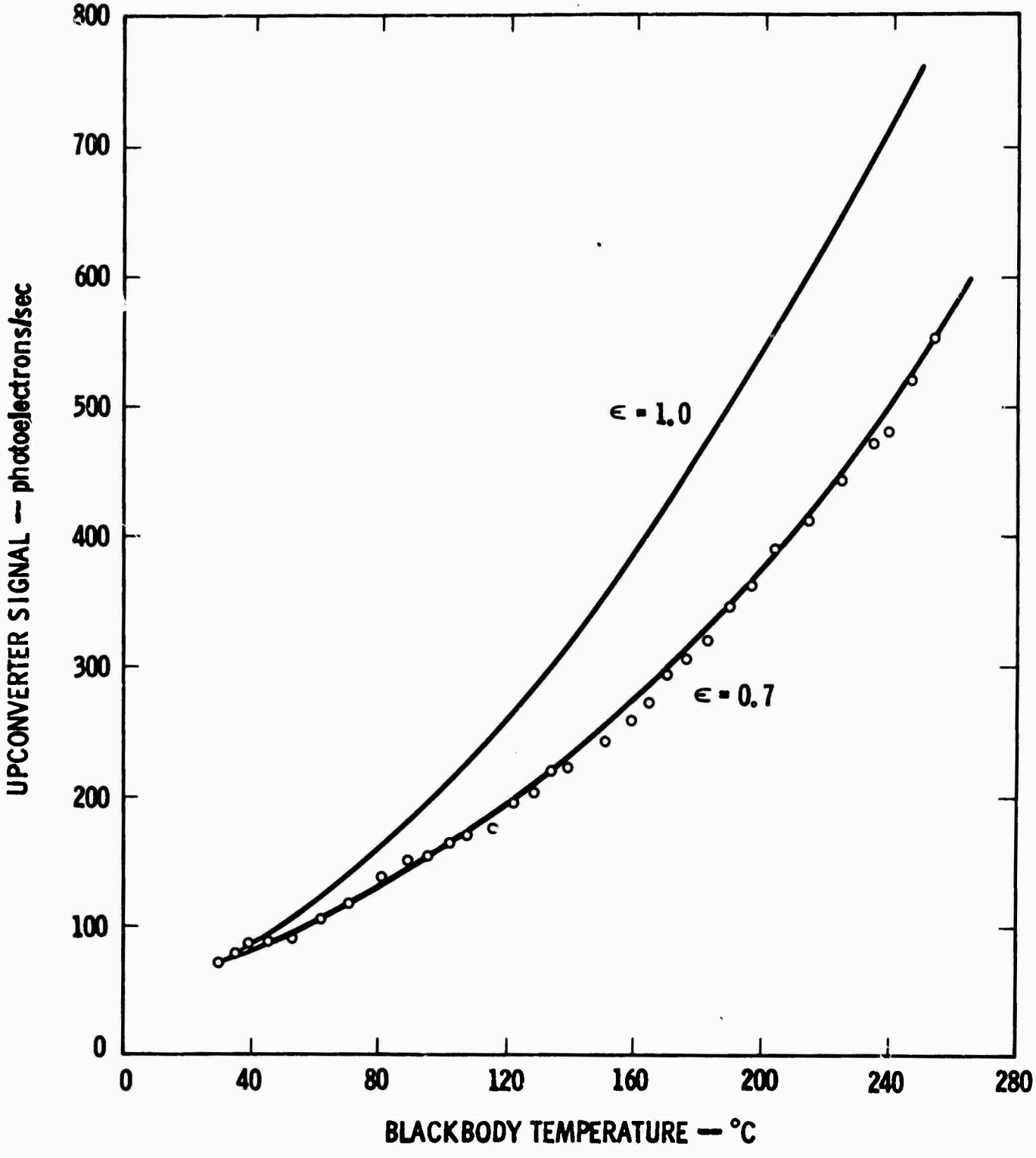

Figure 5-3 Upconverter signal as a function of blackbody temperature. The solid lines are theoretical curves for emissivities of 0.7 and 1.0.

is given by

$$\lambda_{IR} = \frac{\lambda_p \lambda_s}{\lambda_p - \lambda_s}$$

where λ_p is 1.064 microns and λ_s is the measured upconverted wavelength. The upconverter is limited to a long wavelength cutoff of about 12.5 microns due to the absorption in proustite at longer wavelengths.[18] The short wavelength cutoff should be near 1.5 microns. Detection problems prevented extension of the experimentally observed upconverted wavelength below 6.5 microns.

Upconverted signal bandwidths of approximately 70Å were recorded corresponding to the far infrared bandwidths of about 0.7 microns. Using the published dispersion[18] data for proustite it can be calculated[3] that the observed spectral bandwidth corresponds to an infrared radiation upconversion acceptance angle of 6.4° as measured internal to the crystal (full angle).

As a check of the theory developed in this report it is helpful to compare the measured power output with that predicted by Equation (3-16).

For a room temperature thermal image, with $P_p = 0.1W$, $\ell = 0.6$ cm and an external blackbody solid angular acceptance of $7.16 \cdot 10^{-2}$ str. Equation (3-16) predicts an average power output of $2.6 \cdot 10^{-13}$ watts which compares with the measured output of $1.5 \cdot 10^{-14}$ watts (60 photoelectrons/ sec). The difference between the computed upconverter output and that measured experimentally is primarily due to the signal wavelength attenuation of the filter stack used to remove the Nd:YAG radiation from the output of the upconverter.

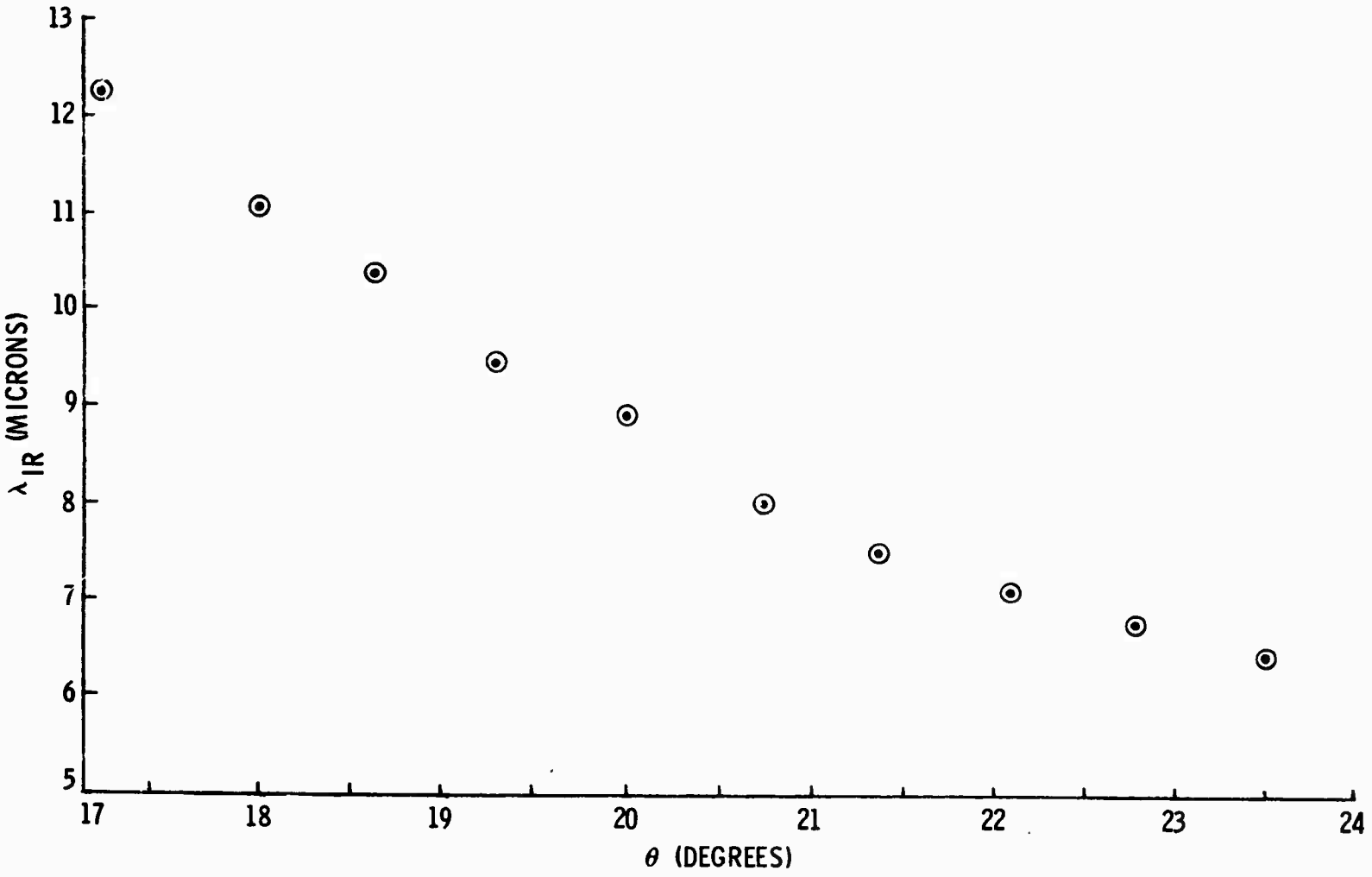

Figure 5-4 Upconverter tuning curve. The crystal is oriented such that its length is 20 deg from the proustite optic axis. The tuning angle is the angle between the direction of propagation of the Nd:YAG laser and the crystal's optic axis. Angles are measured internal to the proustite.

It is interesting to note that the 6.4^{o} full angle, 3.2^{o} half angle, measured upconversion acceptance angle corresponds very nearly to the allowable acceptance angle for an upconverter designed for chromatic abberation-free thermal image detection. An image upconverter so made would have an allowable blackbody acceptance of 3.1^{o} degrees half angle as measured internally to the nonlinear crystal.

Thus the measured signal output power is close to that which would have been available for abberation free upconversion. More precisely $\left(\frac{3.0}{6.4}\right)^{2} \cdot 1.5 \cdot 10^{-14} = 3.3 \cdot 10^{-15}$ watts would have been available from the experimentally investigated upconverter had its angular aperture been reduced to provide for abberation-free imaging.

In this experiment upconversion of room temperature thermal radiation has been demonstrated. The techniques developed have applications similar to those of parametric fluorescence[22]. Thermal upconversion should provide a useful means of determining crystal nonlinearities over a large portion of the optical spectrum. In addition, parametric detection of thermal radiation provides a significant step toward real-time observation of thermal images.

5.3 THE IMAGING UPCONVERTER

It is important to realize that the geometry of the upconverter described above should allow detection of thermal images merely by replacing the phototube by an appropriate image tube. In fact it is noted that the magnitude of the upconverted signal observed from the non-imaging upconverter should be sufficient to detect a 30 element high-contrast, room temperature, thermal image at a 1 cps frame rate.

Observation of a high resolution thermal image depends critically on two parameters of the image tube used to detect the upconverted scene. First the tube must have an equivalent screen background intensity (ESBI) substantially lower than the expected scene energy. The ESBI is the light input that would have been required to produce the background measured in the tube without any actual input. Secondly for good resolution the quantum efficiency of the tube must be as high as possible. The resolution charts given in Figures 3-9 and 3-10 assume unity quantum efficiency and therefore the pump power-time product required for a real imaging system with a given resolution must be increased by $\frac{1}{\eta}$ from those shown in Figures 3-9 and 3-10 where η is the quantum efficiency of the image tube.

The theory of the image upconverter developed in Section 3 of this report shows that the proustite Nd:YAG upconverter viewing a room temperature image should produce $6 \cdot 10^{-13}$ watts of usable upconverted signal for each watt of incident pump radiation. Further since the damage resistance of proustite limits useful Nd:YAG power to about a watt, $6 \cdot 10^{-13}$ watts is the maximum output signal expected from a room temperature thermal upconverter. The measured power output, for 0.1 watt input of Nd:YAG, was $1.5 \cdot 10^{-14}$ watts of which $3.3 \cdot 10^{-15}$ watts was believed to be within the chromatic abberation-free upconverter acceptance angle. Similarly, although the proustite upconverter viewing a thermal scene at 250°C was expected to produce about $6 \cdot 10^{-12}$ watt per watt of pump input, the upconverted power detected was near 10^{-13} watts of which it is believed that $3.3 \cdot 10^{-14}$ watts would be useful for image formation. It is reasonable to expect that these experimentally measured powers could easily be increased by a factor of ten by increasing the Nd:YAG input to 1 watt. A one watt pumped system would

produce a $3.3 \cdot 10^{-14}$ watt image viewing a room temperature blackbody, a $3.3 \cdot 10^{-13}$ watt image viewing a 250°C source. Thus if a 250°C blackbody image is to be detected detector noise must be lower than $3.3 \cdot 10^{-13}$ watts. At present, the only available image detector for the 0.95 micron wavelength region is a S-1 photocathode followed by one or more image intensifiers. The typical S-1 photosurface has an equivalent room temperature input noise of 10^{-9} watts/cm^2 and hence at room temperature is useless as a detector. An S-1 photosurface, cooled to dry ice temperature has an equivalent input noise of approximately 10^{-13} watts/cm^2 and hence might provide marginal detection of the upconverted signal if its beam size were near 1 cm^2.

For reliable detection of any upconverted scene using a cooled S-1 image tube it is probably necessary to gate the tube in synchronism with a pulsed Nd:YAG pump. A gated tube will reduce the effective tube noise by the duty cycle of the gate. Improvement in noise performance of greater than 100 can be expected. Gating of a cooled S-1 image tube, while technically feasible, requires switching of multikilovolt pulses in short time and is difficult and relatively expensive. Further the low quantum efficiency of the S-1 tube, 0.1% at 9600Å implies that even if cooling and gating of the tube were sufficient to reduce its noise to a negligible level, an upconverter operating with a S-1 tube would require 1000 times more pump power to produce the same resolution as an upconverter operating with a unity quantum efficiency image detector.

Rather than experimentally pursue the use of a S-1 image tube in the image upconverter it was decided that use of a InAsP photocathode tube

offered greatest chance of success. The InAsP photosurface, a 3-5 ternary, has been shown to be capable of high quantum efficiencies when deposited in thick layers on InP. Unfortunately requirements for stable image tube performance require a semitransparent, hence a thin cathode.[30] Varian Assoc. under contract to ARPA, (ARPA contract N00014-71-C-0073) was expected to construct such an image tube for our use with the thermal image upconverter. At the start of Varian's program design goals for the image tube were 1) Quantum efficiency of 10% at the unconverted wavelength of 9600Å, 2) Equivalent Screen Background Intensity (ESBI) of less than 10^{-15} W/cm^2 with the photocathode cooled to -68°C, 3) construction of a tube that could be gatable in synchronism with a Q-switched Nd:YAG, i.e., a tube that could be gated on for less than 1 μsec with a 1 KHz repetition frequency.

During the course of the past several months we had the opportunity to attempt use of one of Varian's tubes with the thermal upconverter.

Measurement of the tubes quantum efficiency at room temperature and -68°C were made. Figure 5-5 shows the tube's quantum efficiency as a function of wavelength. Note that nowhere does the tube's response exceed 1%. Varian now better understands the thin InAsP on InP system and currently projects that future image tubes of quantum efficiency no higher than 2-3% should be obtainable.

The ESBI of the Varian tube was made by visually comparing its noise with the noise output of an image tube with a known ESBI. The Varian tube was lens coupled to a RCA 3 stage image intensifier whose ESBI was measured by RCA. With the Varian tube turned off the noise output of the

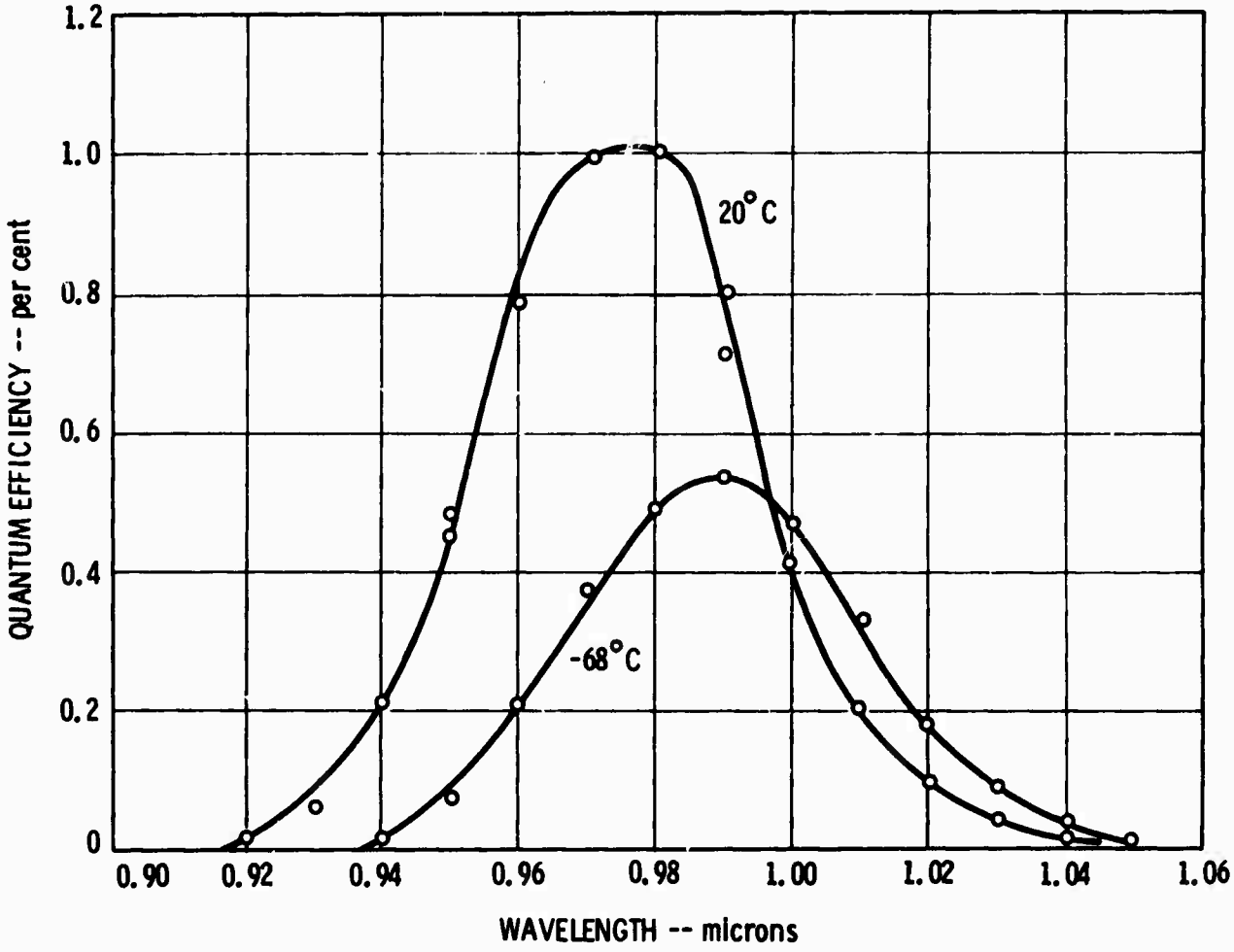

Figure 5-5 Quantum efficiency of the Varian Assoc. InAsP image tube.

RCA intensifier was clearly visible to the dark adapted eye in a carefully darkened room. If the Varian tube was turned on, it was found that at some anode voltage V the image of the Varian tube photocathode became barely visible above the RCA tube noise, i.e., at an applied anode voltage V the tube noise output collected by the lens and imaged onto the RCA photocathode was approximately equal to the RCA tube noise. A shutter was inserted between the Varian and RCA tubes to facilitate this comparison. Knowledge of the Varian tube anode voltage V and its phosphor type (P20) allows calculation of the image tube gain, G. The f number of the collecting lens determines the efficiency of transfer, C, of the Varian image tube noise to the RCA tube. With G and C calculated the ESBI of the Varian InAsP image tube is calculated from

$$ESBI_{Varian} \cdot G \cdot C = ESBI_{RCA} \qquad (5\text{-}2)$$

If the Varian image tube is cooled to $-68^{\circ}C$ the fraction of its noise output collected by the imaging optics equals the noise produced by the RCA tube when the Varian tube anode voltage is 3.5 kV. At that voltage the image tube power gain, assuming $\eta = 1\%$ and a P-20 phosphor, is 3.5. The collection optics, consisting of a f 2.16 lens arranged for 0.85 magnification collects 0.76% of the light incident upon it. The RCA three stage image intensifier has an ESBI of approximately $2.4 \cdot 10^{-14}$ watt/cm^2.

Hence, the Varian tube noise, as calculated from equation (5-2) is $1.3 \cdot 10^{-12}$ w/cm^2. This represents fairly poor image tube noise performance. The measured noise output from the InAsP tube at $-68^{\circ}C$ is more than a order of magnitude greater than that expected from a cooled S-1 tube and 3 orders

of magnitude worse than that initially projected for the InAsP image tube. No quantative attempt was made to measure the noise output of the Varian image tube at room temperature, although it was observed to be appreciably larger than at $-68^{o}C$. In addition to the poor noise performance of the InAsP image tube it was noted the tube intermittently produced purple output flashes of light. These flashes occured most frequently at high anode voltages (greater than 5 kV) or when the anode voltage was changed.

The InAsP image tube supplied by Varian was used in an attempt to detect the upconverted signal produced by the Nd:YAG proustite upconverter.

The image tube was lens coupled to a three stage image intensifier which operated with a gain of greater than 10^4. All attempts at seeing an output image were unsuccessful. Efforts were made to view the system output visually as well as to record it photographically. Inability to record an upconverter output image is reasoned to be due to the excessive noise of the Varian InAsP image. Even with inefficient lens coupling used in the experimental setup the Varian image tube output noise was the dominant system noise. It should be noted that for an image tube with an ESBI of $1.3 \cdot 10^{-12}$ w/cm^2 upconverter output of less than $6.5 \cdot 10^{-11}$ w/cm^2 will not be detectable, i.e., a signal to noise ratio of approximately 5 is estimated to be necessary for detection (Reference 20,21).

The largest experimently produced output was about 10^{-13} watts which, according to the preceeding discussion, should have been large enough to be detected if its beam area was smaller than $1.54 \cdot 10^{-3}$ cm^2 or if its radius were less than .22 mm. The experimental setup was arranged to produce

a signal beam size on the image tube photocathode of slightly less than that size, but the signal output was never seen. Based on the power output measured from the non-imaging thermal upconverter and the measured noise properties of the InAsP tube we surmise that we must have had an image output from the up-converter just slightly weaker than that required to overcome the noise of the Varian image tube. If it had been possible to gate the image tube and employ a Q-switched laser pump, reduction is the average noise would have been achievable and we believe that image detection would have been accomplished. Unfortunately the Varian tube delivered to Sylvania, due to the limited current carrying capacity of its electrodes, could not be gated in synchronism with our Q-switched Nd:YAG laser.

Section 6

ACCOMPLISHMENTS AND RECOMMENDATIONS

The major contributions of this study are three-fold. First a theory of blackbody-image upconversion has been developed which predicts the power output, resolution, contrast and spectral bandwidth from a thermal image upconverter. Secondly, the first detection via parametric upconversion of room-temperature blackbody-radiation was accomplished. Detection of thermal radiation via upconversion provided substantial confirmation of the image upconversion theory, as well as experimentally identifying the image tube characteristics necessary for successful visualization of an upconverted thermal image.

Lastly this study has pointed out the necessary steps to take toward development of an operational 1.06 micron pumped thermal image upconverter. It was shown that the most important upconverter components requiring development are the nonlinear crystal and the image tube or film used to view the upconverter output. In particular, improvement of the nonlinear crystal requires investigation of the causes of crystal damage as well as identification of new nonlinear crystals. Toward these ends, a small effort was directed toward explaining the cw damage mechanism in proustite in terms of its band-edge shift with temperature. Improvement of the image detector required to view the output scene requires not only an increase in the quantum efficiency of available image tubes but more importantly a drastic reduction in their background noise. Alternately, if improvement of image tube technology is not deemed feasible, the upconverter pump wavelength must be changed such that the output image wavelength falls in a spectral region where adequate image detectors exist.

The technology of nonlinear crystals and image tube detectors is currently at the point where available components should be adequate to view a high contrast low resolution scene. If thermal image upconversion is to be used to detect high resolution, low contrast images efforts must be made toward providing a uniform cross section pump beam as well as developing a method of upconverted image contrast enhancement.

SECTION 7

REFERENCES

1. J. E. Midwinter and J. Warner, J. Appl. Phys. 38, 519 (1967).
2. R. C. Miller and W. A. Nordland, IEEE J. Quantum Electron. 3, 642 (1967).
3. J. Warner Appl. Phys. Lett. 12, 222 (1968).
4. J. E. Midwinter, Appl. Phys. Lett. 12, 68 (1968).
5. J. E. Midwinter, IEEE J. Quantum Electron, 4, 716 (1968).
6. J. Warner, Appl. Phys. Lett. 13, 360 (1968).
7. G. D. Boyd, T. J. Bridges, and E. G. Burkhardt, IEEE J. Quantum Electron, 4, 515 (1968).
8. W. B. Gandrund and G. D. Boyd, Optics Communications, 1, 187 (1969).
9. Y. Klinger, F. Arams, Proc. IEEE, 57, (1969).
10. J. Falk and J. M. Yarborough, Appl. Phys. Lett. to be published, Aug. 1971.
11. See for example, G. D. Boyd, E. Buehler and F. G. Storz, Appl. Phys. Lett. 18, 301 (1971).
12. Ronald L. Bell and William E. Spicer, Proc. of IEEE 11, 1789 (1970).
13. A. Yariv, Quantum Electronics, p. 349, (Wiley, New York (1967).
14. I. P. Kaminov and W. D. Johnston Jr., Phys. Rev. 160, 519 (1967).
15. G. D. Boyd and D. A. Kleinman, J. Appl. Phys. 39, 3597 (1967).
16. S. E. Harris, Proc. IEEE 57 2096 (1969).
17. A. Yariv, Quantum Electronics, (John Wiley, New York, 1967) P. 87.
18. K. F. Hulme, O. Jones, P. H. Davies and M. V. Hobden, Appl. Phys. Lett, 10, 133, (1967).
19. See, for example, Papoulis, Probability, Random Variables, and Stochastic Processes, pp. 101, 145, 357, McGraw-Hill Book Co., (1965).

20. A. Rose, J. Opt. Soc. Am 38, 196 (1948).

21. J. S. Parton, J. C. Moody, Image Intensifier Symposium, Ft. Belvoir, Virginia, NASA SP-2 (1961).

22. R. L. Byer and S. E. Harris, Phys. Rev. 168, 1064 (1968).

23. J. Warner, Appl. Phys. Letters 12, 222 (1968).

24. E. O. Ammann and J. M. Yarborough, Appl. Phys. Letter 17, 2333 (1970).

25. W. Bardsley, P. H. Davies, M. V. Hobden, K. F. Hulmer, O. Jones, W. Pomeroy, J. Warner, Opto-Electronics 1, 29, (1969).

26. R. A. Andrews, IEEE J. Quant. Elect. QE-6, 68, (1970).

27. Y. Klinger and F. Arams, Proc. IEEE, 57, 1797 (1969).

28. G. D. Boyd and O. A. Kleinman, J. Appl. Phys., 39, 3597 (1968).

29. D. A. Kleinman and G. D. Boyd, J. Appl. Phys. 40, 546 (1969).

30. R. L. Bell, Photoemissive Detector Semiannual Technical Report, Period of 15 Aug. 1970 - 31 March 1971, ARPA Contract N00014-71-C-0073.

31. G. D. Boyd, W. B. Gandrud and E. Buehler, Appl. Phys. Lett. 18, 446 (1971).

32. J. E. Midwinter and J. Warner, Brit. J. Appl. Phys. 16, 1135 (1965).